Kaunas University of Technology

Faculty of Mathematics and Natural Sciences

Development of Calculation Algorithm for Optimization of Computed Tomography doses based on patient's biometric data

Master's Final Degree Project

VIJAYANAND SIVAKUMAR

Project author

Prof. Dr. DIANA ADLIENĖ

Supervisor

Kaunas, 2021

Kaunas University of Technology

Faculty of Mathematics and Natural Sciences

Development of Calculation Algorithm for Optimization of Computed Tomography doses based on patient's biometric data

Master's Final Degree Project

Medical Physics (6213GX001)

VIJAYANAND SIVAKUMAR

Project author

Prof. Dr. DIANA ADLIENĖ

Supervisor

Prof. Habil. Dr. ARVAIDAS GALDIKAS

Reviewer

Kaunas, 2021

Kaunas University of Technology

Faculty of Mathematics and Natural Sciences

VIJAYANAND SIVAKUMAR

Development of Calculation Algorithm for Optimization of Computed Tomography doses based on patient's biometric data

Declaration of Academic Integrity

I confirm the following:

1. I have prepared the final degree project independently and honestly without any violations of the copyrights or other rights of others, following the provisions of the Law on Copyrights and Related Rights of the Republic of Lithuania, the Regulations on the Management and Transfer of Intellectual Property of Kaunas University of Technology (hereinafter – University) and the ethical requirements stipulated by the Code of Academic Ethics of the University.

2. All the data and research results provided in the final degree project are correct and obtained legally; none of the parts of this project are plagiarised from any printed or electronic sources; all the quotations and references provided in the text of the final degree project are indicated in the list of references.

3. I have not paid anyone any monetary funds for the final degree project or the parts thereof unless required by the law.

4. I understand that in the case of any discovery of the fact of dishonesty or violation of any rights of others, the academic penalties will be imposed on me under the procedure applied at the University; I will be expelled from the University and my final degree project can be submitted to the Office of the Ombudsperson for Academic Ethics and Procedures in the examination of a possible violation of academic ethics.

VIJAYANAND SIVAKUMAR

Confirmed electronically

SIVAKUMAR, VIJAYANAND. Development of Calculation Algorithm for Optimization of Computed Tomography doses based on patient's biometric data. Master's Final Degree Project / Supervisor **Prof. Dr. DIANA ADLIENĖ**; Faculty of Mathematics and Natural Sciences, Kaunas University of Technology.

Study field and area (study field group): Health sciences, Medical technologies (G09).

Keywords: Computed Tomography, Optimization, CT protocols, DRL.

Kaunas, 2021. 49 pages.

Summary

An open-access computational prototype algorithm was developed using MATLAB® for the purpose of optimizing Computed Tomography (CT) examination parameters, based on the biometric data of the patient. The program was developed on the basis of CT dose optimization by the means of Automatic Exposure Control (AEC) systems, as well as international recommendations in this field which were formulated in the past decade. The presented program implements machine-based learning, which after entering the patient's biometric data such as size, shape & age, provides CT Tomography parameters allowing optimization of the doses received by examined patients. The results presented in the work are obtained by testing the functionality of the developed algorithm under different scenarios. The perspectives of practically implementing the program in performing patient Computed Tomography examinations are discussed.

The program was presented at Vilnius University Hospital Santaros Klinikos, Centre of Radiology and nuclear medicine, and was evaluated as a potential tool when performing research on patient dose optimization in Computed Tomography.

SIVAKUMAR, VIJAYANAND Paciento biometriniais duomenimis grįsto kompiuterinės tomografijos dozių optimizavimo skaičiavimo algoritmo sukūrimas Magistro baigiamasis projektas / vadovė **prof. dr. DIANA ADLIENĖ**; Kauno technologijos universitetas, Matematikos ir gamtos mokslų fakultetas.

Studijų kryptis ir sritis (studijų krypčių grupė): Sveikatos mokslai, Medicinos technologijos (G09).

Reikšminiai žodžiai: Kompiuterinė tomografija, optimizavimas, kompiuterinės tomografijos protokolai, DRL.

Kaunas, 2021. 49 p.

Santrauka

MATLAB® platformoje buvo sukurtas atviros prieigos algorito prototipas skirtas kompiuterinės tomografijos parametrų optimizavimui naudojant paciento biometrinius duomenis. Programa buvo sukurta remiantis dozės optimizavimu keičiant automatinės apšvitos kontrolės parametrus (AEC) bei per pastarąjį dešimtmetį parengtomis tarptautinėmis rekomendacijomis šioje srityje. Pateiktoje programoje įdiegtas mašininio mokymosi įskiepis, kuris, įvedus paciento biometrinius duomenis, parenka kompiuterinės tomografijos procedūros parametrus, leidžiančius optimizuoti tyrimo metu paciento gaunamą dozę. Darbe pateikiami rezultatai, gauti testuojant sukurto algoritmo funkcionalumą pagal skirtingus scenarijus. Darbe taip pat aptariamos algoritmo praktinio įdiegimo perspektyvos vykdant paciento dozių optimizaciją kompiuterinės tomografijos procedūrų metu..

Programa buvo pristatyta Vilniaus universiteto ligoninės Santaros klinikose, Radiologijos ir branduolinės medicinos centre, ir buvo įvertinta kaip potencialus įrankis, vykdant pacientų dozių optimizavimo kompiuterinėje tomografijoje mokslinius tyrimus.

Table of contents

List of figures.

List of tables.

Introduction

Clinical imaging has become a fundamental part of diagnosing and treatment of patients, within the present world circumstance. It is now very easier to clinically analyze and restoratively intervene with human anatomy and physiology, with the assistance of ionizing radiation and the advent of modern technologies. Within the final few decades, development in restorative imaging has expanded, beginning with the introduction of computed tomography (CT) in the early 1970s.

Computed tomography (CT) is an imaging strategy that extends the clinical capacities of X-ray imaging. Its tall separation affectability envisions soft tissues and makes tomographic (cut) and three-dimensional (3D) volumetric pictures. It tends to be utilized for a wide scope of clinical applications and it is conceivable to ameliorate images for a wide scope of anatomical regions. This is accomplished by changing a legion of exposure parameters within the clinical protocol elements to provide the vital perceivability of the clinical condition that is being surveyed.

Surveys indicate that CT accounts for almost 60% - 70% of total radiological dose with a never-ending demand [1]. Since its inception, CT technology has been subsequently improved over generations by optimizing various influential technical aspects of it. Since it involves ionizing radiation, patient safety is a primary concern, and steps to ensure it has become the ultimate goal while simultaneously preserving the diagnostic image quality.

In this thesis, different CT optimization trends that have been carried out for the past 10 years were carefully studied, and a solution is proposed by the means of a calculation algorithm. The concept of the program is to simulate different tube current modulation (TCM) approaches based on Effective Diameter and Body Mass Index (BMI) of the patient, and input factors from clinically verified protocols, along with relevant scientific – patient age & size-based tube parameter recommendations. In order to substantiate this concept, the need for a working prototype program is realized. For this purpose, various exposure patterns for a popular series of CT scanners and their TCM was analyzed. 182 clinically verified CT protocols and 17 different CT quantifiers concerning tube settings, dose, and image quality, along with 12 sets of patient-based tube recommendations were programmed into an approximate 5000 lines of fundamental code syntax in a matrix-based programming language. To validate its functionality a total of 9 reference adult & pediatric patients with varying body physique are chosen and 8 different testing scenarios are set accordingly, for head and body CT examinations. Experimentation results of 360 numerical values are then graphically visualized in three dimensional graphs to primarily confirm the basic relationship between different CT parameters, and is discussed in detail to get hold of the advantages and limitations of the prototype. The program is also then demonstrated to clinical professionals to consult the possibility to practically implement the program in a clinical environment.

1. Literature Analysis

Nagel H.D. [2] categorized and briefly discussed the factors that determine the exposure to radiation of patients during a CT procedure. They are mainly grouped into two categories – equipment-related factors and application-related factors. Moreover, the dose due to the CT procedure is described using dose descriptors, which are the Computed Tomography Dose Index (CTDI), Dose – Length Product (DLP). The CTDI being the basic dose descriptor refers to the dose distribution along a line that is parallel to the axis of rotation for the scanner (z-axis) and is recorded for a single rotation of the X-ray source. CTDI can be weighted ($CTDI_w$) or Volumetric ($CTDI_{vol}$) which is pitch-corrected $CTDI_w$. $CTDI_{vol}$ is usually used to assess the radiation output of the scanner and is measured in milligrays (mGy). DLP is the product of the $CTDI_{vol}$ and the Scan length (L). $CTDI_{vol}$ and DLP are the two primary quantities involved with CT.

Current CT technologies offer to achieve the objective of reducing the patient dose, by adapting the dose accordingly to the dimensions of the patient, by various means, namely Automatic Exposure Control (AEC) systems – which is the modulation of the x-ray tube current during scanning [3]. These AEC systems are manufacturer-specific, due to the proprietary algorithms that alter the tube current for each clinical procedure. Notwithstanding, Automatic tube current modulation (ATCM) on CT scanners can yield huge decreases in inpatient dosages. Currently, there is no standard technique for testing ATCM systems [3]. Balance depends on x-ray beam constriction in body tissues from scan projection radiographs (SPRs) or known as 'Scout'/ 'Topogram' and expects to keep up a similar degree of picture quality all through a scan. Noise level is significant in deciding about image quality, however, tissues in bigger patients show higher differentiation coming about because of the presence of fat. CT scanner producers utilize various measurements to evaluate image quality. Some utilize a basic proportion of image noise, while others receive a measure identified with a reference image that acknowledges higher noise levels in even more attenuating leaves behind higher contrast.

Trattner S et al. [4], outlined the roles and responsibilities of clinical and technical professionals involved in the process, of designing a CT protocol to achieve low dose. A CT protocol is a set of parameters that indicate a particular examination, the scanner's technical settings for that specific examination, and contrast delivery necessities if required. These protocols play an important role in deciding the exposure for a patient, and it is generally advisable to design and manage protocols that are tailored to restrain exposure as it were what is required for diagnosis and of practicing patient-focused imaging, and as a result, a set of strategies were formulated to optimize head, chest, cardiac and abdomen CT protocols.

CT protocol administration is one of the foremost investigated regions for the prospect of optimization because it forms the premise of specialized settings that comes about in the dosage exposed to the patient. Zhang et al. [5], created a CT protocol optimization platform by combining task-based perceptibility calculations with a GUI that illustrates the tradeoff between dose and image quality, which can be utilized to make strides individual protocol dosage proficiency, as well as to progress protocol consistency over different patient sizes and CT scanners across large multi-vendor departments with numerous protocol definitions. This work gives a scientific premise for optimization of protocols and helps in keeping up targeted initial detection confidence of lesions at the most reduced radiation dose.

McKenney SE et al. [6], recommended a strategy for CT automatic exposure control (AEC) protocol interpretation between distinctive scanners, objective strategies for changing over tube current modulation protocols among CT scanners were created. Three CT scanners counting a GE LightSpeed 16, a GE VCT, and a Siemens Definition AS+ were examined. Interpretation of the AEC parameters such as noise index and quality reference mAs over CT scanners was particularly examined. A variable-diameter poly(methyl methacrylate) phantom was imaged on the 3 scanners employing an extension of AEC parameters for each scanner. An arrangement of analytic fit functions, compared to diverse patient sizes (phantom diameters), was created from the measured CT information. These capacities relate the AEC metric of the reference scanner, the GE LightSpeed 16 in this case, to the AEC metric of an auxiliary scanner. They found that convention interpretation based on quantitative measurements ($CTDI_{vol}$ or measured image noise) is doable and protocol interpretation includes a reliance on the patient measure, particularly between the GE and Siemens frameworks. Translation plans that protect dosage levels may not deliver indistinguishable image quality.

The CT dose descriptors such as $CTDI_{vol}$ and DLP only indicate the amount of radiation output from the scanner and do not necessarily reflect the amount of dose received by the patient [7]. To overcome this, the American Association of Physicists in Medicine (AAPM) Task Group 204, was formed in 2011, to develop conversion factors to the $CTDI_{vol}$ based on the dimensions of a patient. As a result, the quantifier „Size Specific Dose Estimate (SSDE)“ was proposed for adult and pediatric body examinations based on the 16 cm & 32 cm Poly(methyl methacrylate) (PMMA) phantoms, and a lookup table of conversion factors based on the Anterior-posterior (AP) and lateral (LAT) dimensions of the patient and patient‘s age, were published in the AAPM report no. 204 [8]. Subsequently, a new single curve fit equation was proposed for Adult & Pediatric Head CT examinations, based on the water equivalent diameter (D_w), in the AAPM report no. 293, in 2019 [9]. Moreover, Brink JA et al. [10] provided a clearer review on how the SSDE should be perceived and used in CT patient dose estimation.

One of the interesting studies involving SSDE estimation was that of O’Neill et al. [11], where they evaluated the capability of using the body mass index (BMI) as a size-related metrics alternative to the mid slice effective diameter (D_{eff}) to obtain SSDE in abdominal CT. They demonstrated a very strong correlation between effective diameter and SSDE with BMI, indicating that BMI is an accurate substitute to D_{eff} for SSDE estimation in abdominal CT. A lookup table of conversion factors to calculate SSDE using BMI was published.

Kawashima et al. [12], examined the relationship between the contrast-to-noise ratio (CNR), SSDE, and AEC depending on the patient size, by employing a tissue proportionate material having a human – liver vitality dependence. They found that CNR increments with diminishing phantom size at consistent SSDE, in spite of the fact that the increment proportion is littler than that of the steady CTDI values. Their result demonstrated that the characteristics of the image contrast indeed when the patient dosage gotten from the CT examination is proportionate for individual patient size. Their findings encourage apprehension of the link between CT dosage and image quality based on patient dimensions.

C Anam et al. [13], examined the conceivable outcomes to consequently calculate and after that explore the SSDE in thoracic and head CT examinations attempted utilizing standard imaging

protocols. This was accomplished by computerized calculation of D_{eff} and D_w from patients' images employing a non-user interventional algorithm, and the relationship between Deff and Dw was too examined. Transformation variables were at that point given to calculate Dw from Deff of the patient, for head & thoracic CT. They concluded that, for thoracic examinations, the SSDE diminishes with a diminish in the persistent distance across when AEC is enacted. For head examinations, SSDE increases with a diminished inpatient breadth, in the event that AEC is not actuated.

Additionally, Sarmento et al. [14], compared the adequacy of two diverse patient size metrics based on D_w, the mid-scan water equivalent diameter D_{w_c}, and the mean (average) water equivalent diameter within the imaged locale, D_{w_ave}, for automatic detection of coincidental changes in computed tomography (CT) acquisition protocols. They found that D_{w_ave} could be a superior metric than D_{w_c} for grouping identically sized patients in dosage comparison studies, in spite of the extra algorithmic exertion needed.

Fahmi, A. et al. [15], studied to set up the relationships between D_{eff} & D_w as the premise for calculating SSDE for pediatric head CT examinations. A computer program was utilized to calculate both D_{eff} and D_w from the images of the patients. The D_{eff} and D_w values were related to the age of patients utilizing regression analysis. It was found that these values were related well with the age of the patient. The study moreover established D_w as more accurate as it considers tissue composition and X-ray attenuation in patients [15]. Subsequently, they concluded that the utilize of D_w is best when compared to D_{eff}.

A more up-to-date strategy in precise SSDE estimation is conceivable on the off chance that a slice-by-slice assessment of D_w is made and the tube-current–time product for each CT image is known [16]. When AEC is utilized, and when the patient incorporates a moderately non-uniform conveyance of breadths along the scan length, a more precise SSDE can be calculated than utilizing the easier suspicion of consistent or normal tube current for a filter. For the execution of the proposed concept to be commonsense, an automated computer program was created to extricate the relevant data from the DICOM header on each CT image, and a programmed assurance of the D_w is fundamental for each CT image. They concluded that image and an automatic determination of the Dw are essential for each CT image. They concluded that the proposed procedure holds more potential in exact SSDE estimation when compared to other routine evaluations.

Radiation Dose Index Monitoring (RDIM) framework that permits radiological information collection and patient dosage observing based on DICOM standard empower simple and all-inclusive comprehensive measurements checking for DICOM modalities [17, 18]. RDIM program can extricate exposure information for unsupported documenting and investigation. Closely resembling a Picture archiving and communication system (PACS), Riccardi, L. et al. [19], created a dosage database that might be characterized as a “Dose Archive and Communication System” (DACS). Their study demonstrated the possibility of setting up a multi-institutional organization at a national level pointed at dosage optimization in CT and appeared that sharing insights of dosage records in a multi-equipment setting can be valuable for measurements optimization at an organization level.

Basically, Tsapaki et al. [20], introduced a dosage tracking computer program in a CT department, pointed at assessing the program capabilities and staff execution in an ordinary schedule. All specialized and dosimetric information of 6,010 CT examinations was analyzed. Organ

measurements assessed by the computer program were moreover assessed. It was specified that the computer program gave a straightforward and speedy factual diagram of clinical and specialized information. Ordinary local measurements were comparable to national and worldwide information. Organ dosages demonstrated to be an instrumental and strong instrument in individualized patient dosimetry. The program advertised a simple and fast factual outline of all CT clinical and specialized information and an important outline of workload measurements, which every so often required talk with the staff and, in a few cases, remedial activities. A number of blunders were distinguished, and remedial activities were taken. They concluded that the dosage administration framework demonstrated to be a successful, effective apparatus that encouraged the assessment of common practice and workflow of the CT office and uncovered the propensities of administrators so that remedial activities are made for the advantage of the patient.

Diagnostic reference levels (DRLs) were first mentioned by the International Commission on Radiological Protection (ICRP) in 1990 in its ICRP publication 73 and was subsequently recommended in greater detail in 1996 [21]. DRLs are characterized for a standard-sized patient or phantom and represent a dose level above which it is practical to examine whether a protocol can be improved [21]. However, DRLs are not dose limits, while a dose limit that is not to be surpassed, a DRL can be surpassed if clinical requirements request and is utilized as a trigger to distinguish those facilities utilizing strangely high dosages in a predetermined radiologic technique, for which optimization is required [22].

When optimizing the CT radiation estimations and image quality, there are a couple of viewpoints of the AEC system to consider: the projection points of the localizer, patient situating and centering, protocol assurance, scanning course, and utilization of protective gadgets [23]. Arif Jauhari et al. [24], assessed the impact of mispositioning of patients in connection to the isocenter in CT examinations on the dosage gotten by apparitions with different breadths, for a single set of exposure parameters and found no critical distinction. A situating compensation component gives remedial work when the understanding is off-center; be that as it may, not all CT frameworks are prepared with this component [25]. Furukawa, Y et al. [25] determined a compensation process for empirical-based AEC frameworks to realize an identical impact to that advertised by the component and to confirm the exactness of this process. A relational condition was determined to keep the tube current consistent with varieties in table tallness and quality reference milliampere-seconds (QRmAs), and this was embraced as the proposed emolument strategy. They found that their proposed compensation method enabled the AEC framework to attain ideal tube current and image noise amid patient off-centering.

The Dose Index Registry (DIR) of the American College of Radiology (ACR) is one of the few databases existing with the ACR since 2008 as a portion of the National Radiology Information Registry [26]. The DIR lets facilities compare their CT dosage lists to territorial and national values. The DIR program collects all recorded DICOM components, counting $CTDI_{vol}$ and DLP, for a CT examination. A standardized terminology for the CT protocols was too presented which facilitated the strategy of information collection. The $CTDI_{vol}$, DLP, and SSDE data within the ACR DIR is collected and analyzed on a per-CT method premise and does not collect any patient distinguishing proof data [26]. Numerous other such frameworks were modeled on the premise of ACR DIR and were introduced in nations like UK, Australia, etc. [26].

In the year 2005, MHRA report 05016 authored by N Keat [27], gives a complete understanding of issues surrounding AEC systems in CT and reported on the results of ImPACT's testing on the manufacturers' current systems. The report also discusses the technology and methods of operation of CT AEC systems. Additionally, an examination of AEC frameworks between various makers considering radiation dose and image quality was done as early as 2010. [28]. The purpose of that work was to examine the capability of dose decrease and the likelihood to keep up satisfactory image quality utilizing the AEC systems from four different makers: Siemens Medical Solutions, Philips Medical Systems, General Electric (GE) Healthcare, and Toshiba Medical Corporation. They found that every AEC system is firmly subject to the chosen image quality parameters. Every framework has various arrangements of characterizing the image quality level and thus it is absurd to expect to make a direct correlation between the manufacturers. The dynamic of the tube current modulation is somewhat comparable between the fabricates AEC framework and there is enormous potential for dose reductions. Additionally, a typical outcome is that the image noise increments, particularly in regions where the tube current is significantly diminished by the AEC systems [28].

Also, C J Martin et al. [29] investigated techniques for Automatic Tube Current Modulation (ATCM) procedure on various scanners, think about the alternatives for completing the trial of ATCM systems, and experiences the elements that impact ATCM execution with which administrators should be recognizable. A total evaluation and set of proposals to upgrade ATCM systems were proposed and inferred that it is fundamental that clients of every scanner know about how the ATCM systems on their scanner work and know about the impacts from changing distinctive protocol parameters. Just through individual testing of every scanner with reasonable apparitions combined with reviews of patient doses can the genuine conduct of ATCM systems be completely settled [29].

A recent novel study carried out by Khobragade, P et al. [30], proposes a task-based AEC strategy employing a generalized perceptibility index (d‘$_{gen}$). Their proposed strategy improves existing AEC strategies supported by an endorsed noise level. The generalized metric d‘$_{gen}$ is calculated utilizing lookup tables of the task-based MTF and NPS. They surveyed the execution of the proposed d‘$_{gen}$ -AEC method in giving the specified IQ level over a extend of iterative reconstruction calculations using the ACR phantom with a curved shell and employing a human per user assessment on anthropomorphic phantom images. They concluded that the comes about give preparatory prove that the proposed d‘$_{gen}$ -AEC can deliver comparative IQ over distinctive iterative recreation approaches at diverse measurement levels.

Wang, X. et al. [31], examined the Automatic Tube Potential Selection Component in coronary CTA and found that it was not possible to realize homogeneous objective image quality over the complete patient populace. The effect of the BW and BMI on image quality was not totally disposed of by APSCM. More noteworthy image noise and decreased CNR and SNR were registered in patients with bigger BMIs. They concluded that, clinically, BMI-based tube potential alteration may accomplish a stronger, reliable image quality compared to programmed tube potential determination, especially in patients with bigger body habitus, and thereby settling the irregularity in objective image quality of coronary CTA among different people to a certain degree.

De Mattia, C. et al. [32], broadly assessed four prevalent commercial program applications on CT protocols counting CT-Expo, NCICT, NCICTX, and Virtual Dose. They compared measurement coefficients, evaluated organ measurements and viable dosages gotten by the four program

applications by changing exposure parameters, conjointly compared the comes about with gauges detailed by the computer program creators. They concluded that CT-Expo was the only program subordinate to other exposure parameters, in specific scanner model and pitch, apart from as it were tube voltage and $CTDI_{vol}$ which caused a changeability till 50%.

One of the interesting software for calculating and overseeing radiation dosage of computed tomography for an individual patient is the „IndoseCT“ created by Choirul Anam et al. [33], which gauges the $CTDI_{vol}$ for most of the scanner models, and it calculates the SSDE of the patient, as well as the assessment of connections between D_w and average tube current. Their study showed that the rate contrasts between calculated and reported $CTDI_{vol}$ values were less than 10%. They illustrated how SSDE can be evaluated utilizing average tube current and the water-equivalent distance across D_w. This software is also utilized in this work to obtain the $CTDI_w$ values for SIEMENS scanners.

Similarly, Mubarok S et al. [34], created an Android™ based computer program for evaluating CTDIvol and image quality measures through a extended of varied exposure parameters. CTDI estimations were performed utilizing PMMA phantom of 16 cm breadth, whereas the image quality test was conducted by utilizing Catphan® 600 phantom. Image quality assessed through CNR parameter with most extreme distinction to real CNR estimation of 21.65% [34]. Other commercial software for the purpose of dose management available is the Qaelum DOSE [20], the Affidea Dose Excellence [35], and the GE DoseWatch [36].

The 2019 report by the State Health Care Accreditation Agency of the Health Ministry of Lithuania, gives away the current statistical analysis of the CT equipment being used in Lithuania [37]. According to the Accreditation Services 2019, in a total of 73 CT scanners, 61 CT are used in Lithuanian public health institutions and 12 in private facilities. Most of the CTs are installed and used in the 3 largest in Lithuanian counties: 24 in Vilnius, 14 in Kaunas, and 11 in Klaipėda. 35 CT were operated (47%) produced more than 10 years ago (during 2002–2009), 20 CT (27%) (during 2010-2014), and 19 CT (26%) were produced in the last 5 years (during 2015–2019). Around 28 scanners are 16 slices, and 15 are 64 slices, and 9 are 128 slices. The data of the Lithuanian Department of Statistics on the population of Lithuania states that Lithuania has an average of 2.6 CT devices per 100,000 population.

Based on the comprehensive literature analysis carried out, the purports of the thesis were well established in the direction of optimization of patient dose resulting due to CT procedures, should consider the biometrics of the patient into account, which includes the factors such as size, age, BMI, circumference, etc. The significant roles played by clinical protocols, DRLs, AEC & ATCM systems and their inclusion in optimizing procedures is also recognized.

The aim of this particular work was to develop a calculation program that provides an optimization plan for a head/body CT examination, by considering an adult/pediatric patient's biometric data. It provides a comparison between results, mainly $CTDI_{vol}$, SSDE and CNR values, arising from protocol recommended kV_p & mA values and different TCM approaches involving patient's D_{eff} & BMI. It also acts as a platform to check if these results are in accordance with the National and International DRL values for the chosen procedure. This program is created with the intent of using it as a research tool, by medical physicists working in hospitals, enabling them to visualize the optimal kV_p & mA values that needs to be set, for the patient, without compromising the image quality. To achieve the prime objective of this work, the following tasks were set,

1. To analyze commercially available CT dose optimization and management software programs, in the market, and prevailing trends.
2. To create a prototype of the program using a suitable programming environment namely MATLAB®, using a simple script based execution format.
3. To validate the program's proper execution and functionality with different testing scenarios comprising of several reference patients and protocols.
4. To discuss the outcomes of this testing.

2. Materials and Methods

In this section, the fundamental working principle of the SIEMENS CARE Dose 4D ATCM system is briefly explained. Following that the different parameters involved and the flowchart of the BioptiDOS program is explained concisely.

2.1. Overview of the SIEMENS CARE Dose 4D system

The essential rule behind an ATCM framework is to adjust tube current to attenuation of body locale, where tube current is consequently expanded for more scattering locale and vice versa without diminishing the image quality [2]. These ATCM frameworks can utilize varied strategies such as tweaking the tube current either longitudinal, angular, temporal, or all those combined [2, 38].

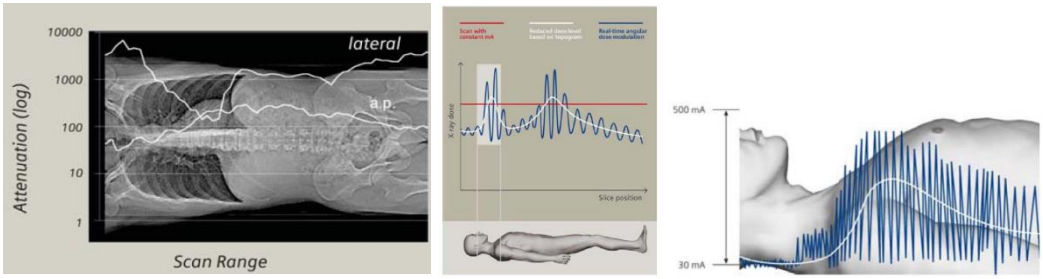

Fig. 1. Illustration of SIEMENS CARE Dose 4D ATCM system [28]

The combined ATCM framework utilized within the SIEMENS (Erlangen, Germany) CT scanners is named CARE Dose 4D ©. The framework alters the tube current concerning the patient's dimensions in conjunction with spontaneously adjusted tube current modulation amid every tube turn [28]. Based on the CT - "Scout/Topogram" images gotten from the localizer, AP or LAT scattering profile along the z-axis is measured assessed for the perpendicular heading with an empirical condition. Tube current (axial) values are decided from the estimation of these attenuation profiles. The relationship between tube current and attenuation outline is once more characterized by an expository work for slice position within the z-axis and alter the tube current to the dimensions of the patient and constriction changes (longitudinal modulation). Balance of tube current is based on the administrator chosen Quality Reference mAs and is very preternatural to protect required image quality along with the scanning course [28].

MacDougall et al. [39], derived the empirical equation employed by the CARE Dose 4D system, which is given as follows,

$$\frac{\textbf{Effective mAs}}{\textbf{Quality Reference mAs}} = e^{(D-D_{Ref}).S} \quad (1)$$

The components of the equation are given in the following table.

Table 1. Components of the CARE Dose 4D empirical equation [39]

Effective mAs (Pitch corrected mAs) - **mAs_{eff}**	$\left(\frac{\text{Tube Current (mA)*Rotation time (sec)}}{\text{Pitch}}\right)$
Quality Reference mAs - QRM	QRM is defined as the nominal effective mAs for the reference patient. With the setting of the "Image Quality Reference mAs," the user may adjust image quality

	(image noise) to the diagnostic requirements and the individual preference of the radiologist. The QRM is not adjusted for patients' size.
D – Effective diameter	Effective diameter (or) patient equivalent diameter.
D_{ref} – Reference diameter	The diameter of the reference phantom.
S	Constant values derived to match CARE Dose 4D modulation strengths. (0.06 – weak, 0.10 – average, 0.17 – constant noise)

The quality reference mAs value, which is chosen by the administrator, ought to be supported by the demonstrative prerequisites of a chosen protocol and the personal inclination of the facility, and it is not modified for patients of different sizes. For each protocol, QRM demonstrates the mean effective mAs. The administrator then chooses a commonplace value that represents a reference patient, characterized as a grown-up with a weight of roughly 70 to 80 kg. For pediatric protocols, the effective mAs ought to be chosen for an ordinary child with a weight of 20 kg. In this way, CARE Dose 4D alters the tube current for each revolution. QRM is then set according to the attenuation at the z-axis comparative to the size of the reference patient [28]. The framework decides if the patient is a little "slim" or huge "obese" from the scout/Topogram images. The amount of alter in tube current chooses to agree to the modulation strength indicated by the administrator. For thin patients/regions, powerless, normal, or solid balance settings will result in a powerless, normal, or solid diminishes in radiation measurements, individually as appeared in Table 2. Söderberg et al. [40], examined the impact of these adjustment qualities with a chest human apparition and found a significant decrease within the radiation measurements employing a fixed tube current. They moreover found a significant distinction within the image quality between the adjustment qualities and concluded that the adaptation strengths can be utilized to get user-specified alterations to image quality or radiation exposure to the patient.

Table 2. CARE Dose4D strength settings and its effects on Tube current [40]

Patient size	**Weak**	**Average**	**Strong**
Thin	Little reduction	Moderate reduction	Sharp reduction
Fat	Little increment	Moderate increment	Sharp increment

2.2. Overview of the BioptiDOS program

In this program the user would be able to simulate the different possibilities of optimizing the dose, by referring to clinically approved protocols, national, institutional, and local DRL values to make sure that the simulated values are on lines with the conventional values. This might be skipped if the patient has any peculiar clinical needs. The results of each simulation are then stored in an inbuilt database, which the program refers to, for successive simulations of the same procedure.

For the purpose of a prototype program, a MATLAB® program was written using MATLAB – R2020b v.9.9.0 (The MathWorks Inc.), incorporating various functions [41]. The Master code for this program is provided in the Appendix section. Currently, this program can be used only for the SIEMENS CARE Dose4D system, as it is the only empirical algorithm, where the target noise is varied over the patients' size [42], whereas systems used by other manufacturers like General Electric, Phillips, Toshiba, are based on the aspects like Noise index, Reference image, and Standard Deviation of pixel values, respectively [42].

2.2.1. Quantifiers

The different quantifiers used in this program are given in the following Table. 3, along with their brief respective definitions.

Table 3. Quantifiers used in the program

Sl.no.	Quantifier.	Definition.
1.	**Tube voltage (kV_P)**	Tube potential is the electrical "potential" difference between the electrodes of the x-ray tube and is measured in kilovoltage [43].
2.	**Tube current (mA)**	Tube current decides the intensity of the electrons striking the anode, which primarily affects the number of emitted x-ray photons. It is measured in milliamperes [43].
3.	**Rotation time (sec)**	The time is taken for gantry rotation in a helical CT scan, which is measured in seconds.
4.	**Detector collimation (mm)**	The length of the individual detector acquiring data for each of the simultaneously acquired slices that limit the width of the x-ray beam contributing to that slice is often referred to as detector collimation [44].
5.	**Slice thickness (mm)**	Slice thickness refers to the resolution of the scan, which is the size of the individual components of the detector array.
6.	**Pitch**	It is the ratio of the patient table feed to the total nominal beam width for a CT scan.
7.	**Computed Tomography Dose Index CTDI (mGy)**	The CTDI is the basic quantifier specific to CT modality and is derived from the dose distribution along a line that is parallel to the z-axis and is recorded for a single rotation of the source. Weighted CTDI ($CTDI_w$), which represents the CTDI averaged over the cross-section of the phantom and Volumetric CTDI ($CTDI_{vol}$) is the pitch-corrected $CTDI_w$ [2].
8.	**Dose Length Product DLP (mGy-cm)**	It is the product of $CTDI_{vol}$ and the scan length [2].
9.	**Anterior – Posterior Length (AP)**	Distance between the farthest points of anterior and posterior anatomical sections of the human body.
10.	**Lateral length (LAT)**	Distance between the farthest points of anterior and posterior anatomical sections of the human body.
11.	**Effective diameter (D_{eff})**	It is the squared root of the product of AP and LAT body dimensions.
12.	**Water Equivalent Diameter (D_w)**	For the x-ray scattering of a patient in terms of a water cylinder having the same x-ray absorption, its diameter is referred to as water equivalent diameter (D_w) [45].

13.	**Size Specific Dose Estimate SSDE (mGy)**	Size Specific Dose Estimate is the product of $CTDI_{vol,}$ and conversion factor based on the effective diameter and the reference phantom [8]. The conversion factors required for its calculation are provided in the Appendix.
14.	**Contrast-to-Noise-Ratio (CNR)**	Image quality can be represented CNR, which is just the ratio of the estimated contrast and noise, in the region of interest (ROI). **CNR =** $\sqrt{(0.01966\ CTDI_{vol} + 0.11167)}$ **x Slice thickness** [34, 46].
15.	**Relative Dose Factor (RDF)**	RDF is utilized as a quantifier as to what division of the dosage that a given tube potential must give the same CNR as a reference tube potential [46, 47]. $\mathbf{RDF} = \left[\frac{\text{CNR ref}}{\text{CNR i}}\right]^2 * \left[\frac{\text{Dose i}}{\text{Dose ref}}\right]^2$ -where *i* is a given combination of tube potential and tube current suggested by the AEC and *ref* corresponds to that of the protocol [44, 45].
16.	**Diagnostic Reference Levels (DRLS)**	Most commonly used dose indices such as $CTDI_{vol}$ and DLP are used as reference values from international, national, and institutional facilities for a given procedure.
17.	**Body Mass Index (BMI)**	BMI is a value derived from the weight and height of a person. Based on the values, a person can be categorized as less weight, normal, overweight, and obese [48]. $\mathbf{BMI} = \frac{\text{weight (kg)}}{(\text{height (m)})\text{^}2}$

2.2.2. Scanners

The SIEMENS Sensation 16 Slice CT and 64 slices CT scanners are among the most popular multi-slice, full-body best-selling CT scanners available. Presently, the prototype program is modeled for use with SIEMENS Sensation 64 and Sensation 16 scanners. To simulate the SIEMENS CARE Dose 4D system for these two scanners, the $CTDI_w$ output for different scan settings must be known. To achieve this, the proprietary "IndoseCT" software which was developed by Choirul Anam et al. [33], was used.

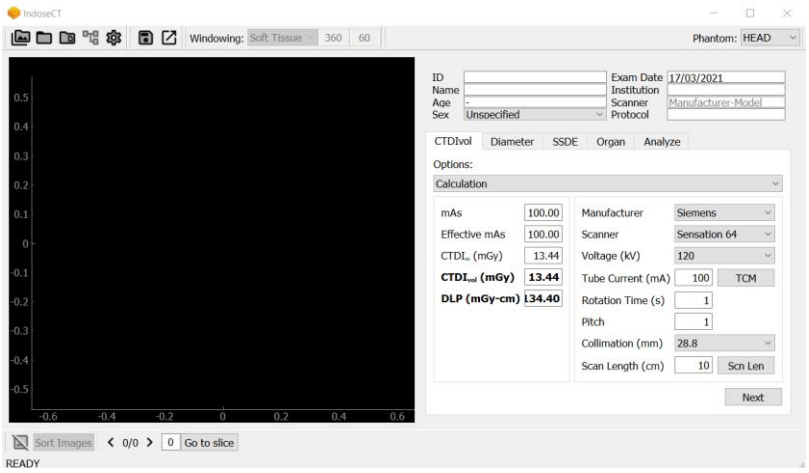

Fig. 2. The window of IndoseCT software

Different factors such as tube voltage, detector collimation, rotation time, phantom (head/body), influences the $CTDI_w$. The $CTDI_w$ for a given tube voltage and current, detector collimation, rotation time, phantom (head/body), for the selected scanner was obtained using the software and was plotted as a straight line as shown in Fig. 3. (a) and (b). The straight-line equations were then used to obtain $CTDI_w$ values using the k_{CTDI} values from the lookup Tables. 4 and 5 and multiplying the desired tube current values.

$$\mathbf{CTDI_w = k_{CTDI} * Tube\ current\ (mA)} \quad (2)$$

if k_{CTDI} is a constant.

Table 4. k_{CTDI} values for Sensation 16

Scanner	**Phantom**	**Tube potential (kV)**	**Collimation (mm)**	**kCTDI**			
				Rotation time (sec)			
				<0.5	**0.5**	**0.5-1.0**	**1**
Sensation 16	Body	80	0.5	0.0082	0.0135	0.0203	0.0271
			0.75	0.0076	0.0127	0.091	0.0254
			1.5	0.007	0.0117	0.0175	0.0233
		100	0.5	0.0166	0.0278	0.0416	0.0554
			0.75	0.0156	0.026	0.039	0.052
			1.5	0.0143	0.0238	0.0358	0.0478
		120	0.5	0.0263	0.0438	0.0658	0.0877
			0.75	0.0247	0.0411	0.0617	0.0823
			1.5	0.0226	0.0378	0.0566	0.0755
	Head	80	0.5	0.0244	0.0406	0.061	0.0813
			0.75	0.0229	0.0381	0.0572	0.0762
			1.5	0.021	0.035	0.0525	0.0699
		100	0.5	0.0465	0.0774	0.1161	0.1548
			0.75	0.0435	0.0726	0.1089	0.1452
			1.5	0.0399	0.0666	0.0999	0.1332
		120	0.5	0.0642	0.107	0.1606	0.2142
			0.75	0.0602	0.1004	0.1506	0.2009
			1.5	0.0553	0.0922	0.1382	0.1842

Table 5. k_{CTDI} values for Sensation 64

Scanner	Collimation (mm)	Phantom	Tube potential (kV)	kCTDI			
				Rotation time (sec)			
				<0.5	0.5	0.5-1.0	1
Sensation 64	0.4	Body	80	0.005	0.0084	0.0126	0.0168
			100	0.0114	0.019	0.0286	0.0381
			120	0.0195	0.0325	0.0487	0.065
		Head	80	0.0144	0.019	0.0286	0.0381
			100	0.0242	0.0403	0.0605	0.0806
			120	0.0403	0.0672	0.1008	0.1344

It is evident from plot Figure 3. (a) and (b) that, with the increase in tube voltage and current, $CTDI_w$ which is the tube output, linearly increases, for a given rotational time of 1 second. Also, the dose is higher for a head phantom (16 cm), when compared to a body phantom (32 cm), for the same conditions. These $CTDI_w$ calculations form the basis of the program.

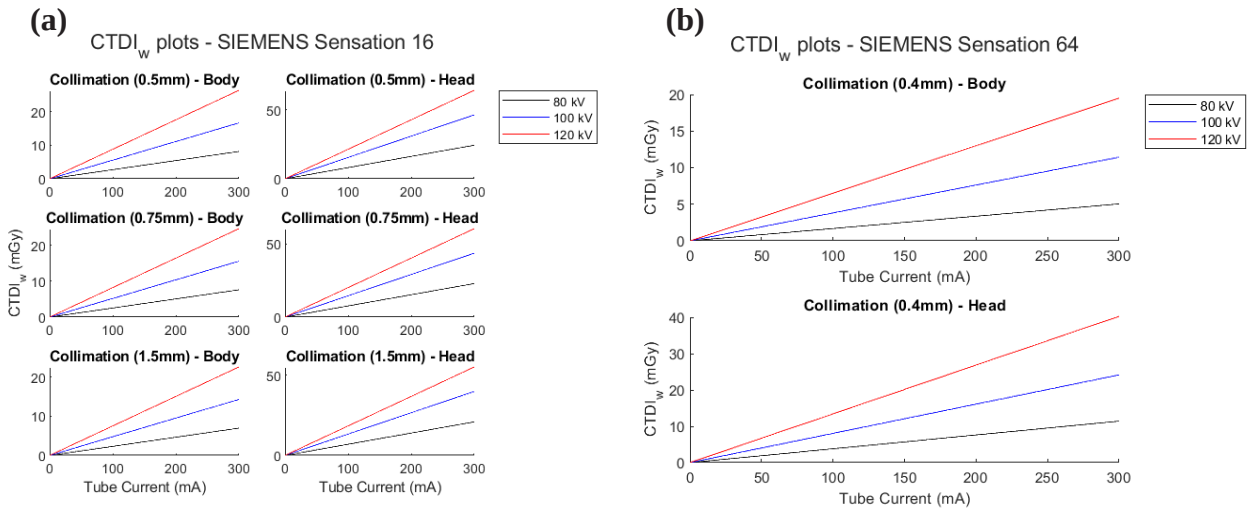

Fig. 3. (a) $CTDI_w$ plots for Sensation 16 & **(b)** $CTDI_w$ plots for Sensation 64

2.2.3. Protocols

The clinical Adult and Pediatric CT protocols for Sensation 16 and 64 scanners, required for the program were obtained from the popular, open-source website for CT-related information - „CTisus“ which was developed by Elliot K. Fishman, M.D. of the Johns Hopkins University [49]. Additionally, access to various other vendor-independent clinical protocols from renowned clinical institutions and websites such as vRad, UT Southwestern Medical Center, Lifespan by Rhode Island Hospital and The Miriam Hospital, Oregon Health & Science University, TRA Medical Imaging, and Dartmouth Geisel School of Medicine was also provided [50 – 55]. Each protocol was assigned a unique ID, for

the integration of data for protocol optimization purposes, and protocol-wise DRL tracking and benchmarking purposes. A total of 182 CT protocols were embedded in the program and are listed in Table A1. given in the Appendix.

2.2.4. Size and age-based tube parameters recommendations

Different recommendations for a given procedure were generated for a given procedure, based on the findings of various researchers, and conventions followed by reputed clinical institutions. These recommendations have been proven to yield better results without much exposure to the patient, thereby ensuring patients' safety. Some of the important recommendations are given below.

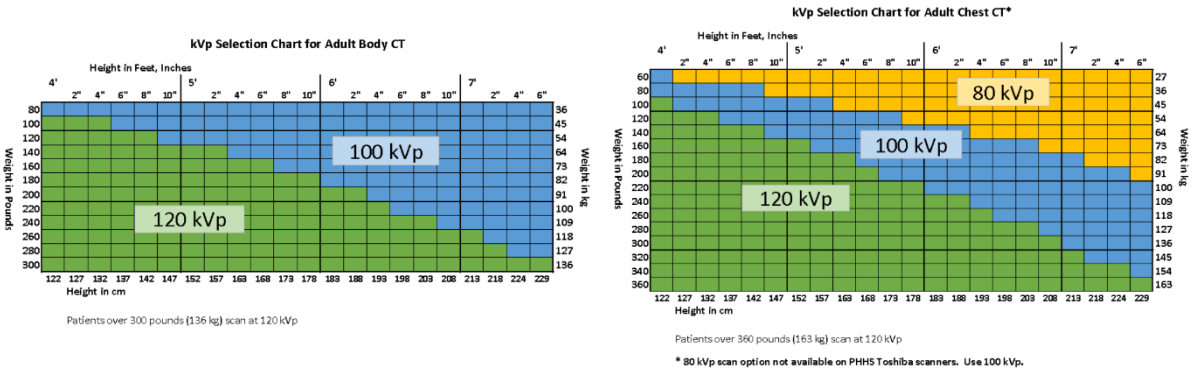

Fig. 4. kV_p selection chart used in UT Southwestern [51]

A set of recommendations were provided for pediatric procedures based on the Lateral width and abdominal circumference [39, 56], which is given in the following table.

Table 6. Pediatric protocol recommendations

Phantom	**Lateral width (cm)**	**Effective mAs**	**kV based on Lateral width**	**kV based Abdominal circumference**
32	<=15	150	80	120
32	16 – 25	175	80	120
32	26 – 35	175	100	120
32	>36	135	120	120
	Pediatric Weight		**kV based on Pediatric weight**	
16	< 40	-	80/100	80
16	> 40	-	100/120	80

The tube current range allowed for body CT procedures, based on Lateral width was proposed by McCollough CH et al. [42], as follows,

Table 7. Maximum and Minimum Tube current range

Lateral width (cm)	**Minimum mA**	**Maximum mA**
22.1 – 30	150	280
30.1 – 40	220	500

40.1 – 45	400	720
45.1 – 50+	450	770

The program was designed in such a way that, the relevant recommendations are displayed appropriately based on the biometrics of the patient, given as the input. This lets the user, choose the correct parameters along with the protocol recommendations.

2.3. Diagnostic Reference Levels (DRLs)

The definition, standards, and the role of DRL values in CT Dosage optimization, and the requirements for DRL values tracking and benchmarking were broadly examined by different authors [57 – 60]. One of the most highlights of the program is to supply the client with established DRL values for a particular procedure to make a culture of patient dosage mindfulness, and to realize this, the most recent international and national DRL data were collected [61 – 66].

The DRL information is accessible for both grown-up and pediatric patients and is assembled for the foremost common CT examinations covering the three primary anatomic locales, the head, abdomen, and chest CT. The DRL data used in the program is given in the following table.

Table 8. DRL information

Age	**Region**	**International DRL**		**National DRL**		**$CTDI_{vol}$ Alert values (mGy)**
		$CTDI_{vol}$ (mGy)	**DLP (mGy.cm)**	**$CTDI_{vol}$ (mGy)**	**DLP (mGy.cm)**	
Adult	Abdomen	18	665	-	1200	-
	Pelvis	14	525	-	506	50
	AP	15	641	-	-	-
	Head	54	854	-	650	80
	Chest	12	449	-	910	50
	Thoracic	-	-	-	680	
	Cardiac	-	-	-		150
	Lumbar Spine	-	-	-	600	-
	Cervical Spine	-	530	-	-	-
Pediatric						
<= 1 year	Abdomen	5.2	130	-	-	10 (32 cm)
1 – 5 years		7	250	-	-	25 (16 cm)

5 – 10 years		7.8	310	-	-	-
<= 1 year	Head	26	440	-	570	-
1 – 5 years		36	540	-	630	60
5 – 10 years		43	690	-	650	-
<= 1 year	Chest	5.2	130	-	-	10 (32 cm)
1 – 5 years		6	140	-	-	25 (16 cm)
5 – 10 years		6.8	170	-	-	-

For a chosen procedure, the relevant DRL data is displayed in the form of histograms in conjunction with numerical values. The institutional and local DRL values are shown within the shape of boxplots so as to know the diverse ranges (mean, median, quartiles) of DRL values for all the age groups. In spite of the fact that this DRL data is more generalized values for a given procedure, and it has been well elucidated by the ICRP [21], that DRLs are collected for reference patients, and does not truly mean as a “barrier” for dosage from a clinically justified procedure for a patient, that surpasses the DRL for that particular procedure. Additionally, this convenient reference to existing DRL values empowers the user to keep track of the patient dose and to optimize a given protocol appropriately.

2.4. Workflow of the program

For the purpose of the prototype program, a navigational simple script-based MATLAB program was written. Also, it is not possible to alter the once-fixed parameters to tweak the final results. This can be justified by the extensive lines of code that are required to run the program each time. Since the data from previous iterations gets stored and checked with the successive ones, it was almost impossible to add the mentioned feature. But when developed as a complete software the time-consuming navigational nature can be eradicated and a single dialog window approach can be implemented, ensuring quick operation and the simulative feature can also be added. The following flow chart describes the functioning of the program.

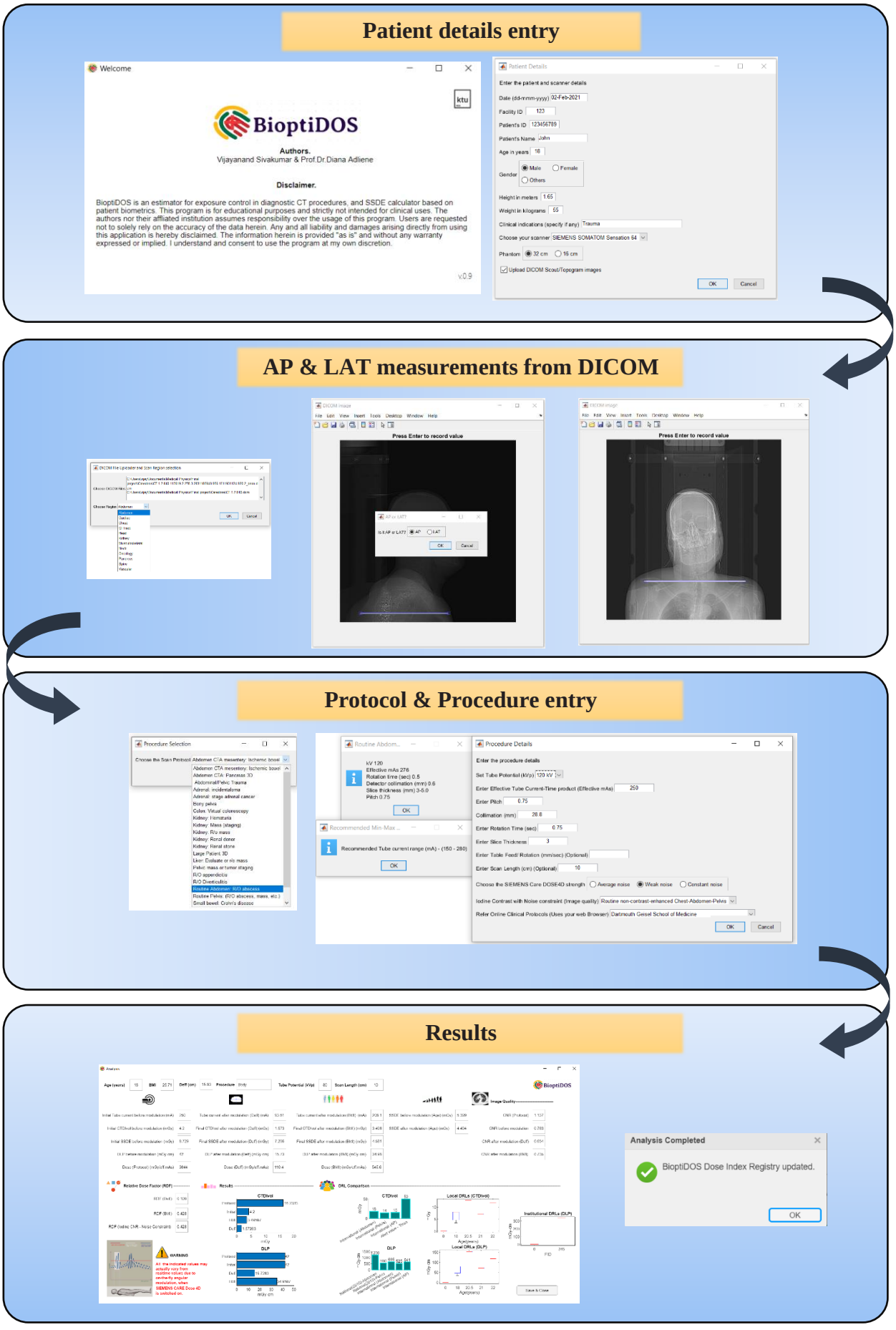

Fig. 5. Workflow of the BioptiDOS prototype program

The following workflow has been proposed,

- The patient details such as patient-specific ID number, name, age, gender, height, weight, clinical indications, along with facility ID, scanner information namely scanner model, phantom (32 or 16 cm), are entered in the first dialog box. The option to upload DICOM Scout / Topogram images taken prior to the actual scan is also added for AP and LAT measurements.

- Based upon the user selection to upload DICOM images, the consecutive dialog box is opened. If the option is not selected, the user can then manually enter the AP and LAT dimensions in the next window. If the option is selected, a dialog box opens where the DICOM files required are chosen through a file explorer window. Additionally, at this step, the user is required to choose the scan region of the examination (Abdomen, Head, etc.).

- Once the files are chosen, the user then manually adjusts and selects the farthest points between the projected image of the patient's body. Based upon the orientation of the image, the dimension is entered upon the confirmation dialog box that appears once the measurement is over.

- After the measurement of AP & LAT is completed, the scan protocol is chosen. This is based on the scan region that was chosen in the previous steps. The list of protocols available for the chosen scan region is displayed as a list drop-down dialog box. The user then chooses the appropriate protocol for the examination.

- Based upon the protocol selection, several dialog boxes are opened after the previous step. These dialog boxes contain the recommendations based on the chosen parameters and the patients' information. The foremost one has the protocol recommendations including tube parameters, slice thickness, rotation time, collimation, etc., Other dialog boxes contain individual suggestions based on the age, height, weight, abdominal circumference of the patient.

- Once the recommendations are shown, simultaneously the procedure selection dialog box appears, where the actual parameters are entered by the user based on the recommendations shown by the program. This procedure selection box includes options to set tube voltage & current, pitch, rotation time, collimation, slice thickness, scan length, CARE Dose 4D tube current modulation strength (the function of the ATCM system to set image quality), etc. Also, an option to choose the other online protocols is given. When selected, the website page with protocols is opened in the system default browser.

- Following the procedure selection step, the program then calculates all the required data to be shown to the user. The results are displayed in a large window with bar charts. The results include mean tube current of the CARE Dose 4D system, $CTDI_{vol}$, DLP, SSDE based on the effective diameter/water-equivalent diameter, age, dose per mAs, CNR, RDF, for protocol, size-based, and BMI based altercations in separate columns. Finally, the results are plotted on horizontal histograms, and the international, national, institutional, and local DRL values for the same procedure are shown as histograms and boxplot charts.

- Once the user visualized the data, the "Save & Close" button is pressed, where the data of that particular trial is saved in the inbuilt data tables for future references. These data tables are known by the name "BioptiDOS Dose Index registry". This is data is used in successive trials of the program.

2.5. Validation of functioning

In order to validate the proper functioning of the program, the program was tested for different simulated trials for patients of diverse parameters (age, size), for both the head and body examinations, for both the scanner models programmed, which are the SIEMENS Sensation 64 and 16 CTs. A total of 9 patients of varying bodily proportions and age were considered for this purpose. Table. 9 describes the characteristics of the patients and the protocols used in this study are given in Table. 10. The results of the validation trials are discussed in the next results and discussion section.

Table 9. Patient characteristics

Patient ID	**Age (years)**	**Gender**	**Height (m)**	**Weight (kg)**	**BMI**	**D_{eff}**
001	1	M	0.7	10	-	10.6
002	2	M	0.80	14	21.9 (obese)	18.1
003	2	F	0.86	12.5	16.6 (healthy)	16.5
004	5	F	1.06	16	14.2 (healthy)	13.8
005	11	M	1.44	42.9	20.6 (overweight)	24.6
006	11	M	1.42	27.6	13.7 (lean)	20.9
007	21	M	1.70	65	22.5 (healthy)	16.5
008	23	M	1.75	67.1	21.8 (healthy)	34.5
009	23	F	1.69	50	17.5 (lean)	32.5

Table 10. Protocols used

Scanner	**Protocol ID**	**Protocol Name**	**kV**	**mAs_{eff}**	**t_{rot} (sec)**	**Col.**	**Slice thickness**	**Pitch (TF for Sensation 16)**
Sensation 64	S64A118	Routine Abdomen: R/O abscess	120	276	0.5	0.6	3	0.75
Sensation 64	S64P11	Abdomen	120	60	0.33	0.6	1.5	2.5

Sensation 64	S64A55	R/O Bleed (Routine Spiral)	120	400	1	0.6	0.75	0.8
Sensation 64	S64P41	Head CT (Routine Spiral)	120	175	0.33	0.6	1	0.65
Sensation 16	S16A11	AbdRoutine (R/O abscess, FUO, etc.	120	200	0.5	1.5	3	24.0
Sensation 16	S16P12	Routine study (ie. r/o abscess, mass adenopathy)	120	30-40	0.5	1.5	5	24.0
Sensation 16	S16A33	Head/Neck (Angio head)	120	200	0.5	0.75	0.75	6.8
Sensation 16	S16P46	Routine Head Study (Spiral)	120	150	0.75	1.5	5.0	11.8

3. Results and discussion

The results of the validation trials briefed in the previous sections are given in Table 11, as follows,

Table 11. Trial results

Scanner	Procedure	Patient	kV	mAseff			CTDIvol (mGy)			SSDE (mGy)			SSDEage (mGy)		DLP (mGy.cm)			CNR				RDF		DRL	
				Initial	Deff	BMI	Initial	Deff	BMI	Initial	Deff	BMI	Before	After	Initial	Deff	BMI	Protocol	Initial	Deff	BMI	Deff	BMI	CTDIvol	DLP
Sensation 64	Body	2M	80	454.5	523.4	829.6	2.0	2.3	3.7	1.9	3.4	5.3	2.1	3.8	20.7	23.8	37.8	0.61	0.47	0.48	0.52	0.6	1.2	7	250
		2F	80	378.8	383.5	543.3	1.72	1.74	2.4	1.7	2.4	3.9	1.7	2.5	17.2	17.4	24.7	0.58	0.46	0.46	0.49	0.4	0.8	7	250
		11M	120	405	206.3	194.9	17.5	8.9	8.4	30.1	14.5	14.1	27.8	13.4	175.5	89.3	84.4	1.17	1.17	0.92	0.91	-	-	18	1200/665
		11M	120	405	258.2	268.1	17.5	11.1	11.6	26.2	17.3	16.9	27.8	18.4	175.5	111.9	116.2	1.17	1.17	0.99	1.01	-	-	18	1200/665
		23M	120	414	485.1	289.8	17.9	21.0	12.5	18.4	12.9	17.9	-	-	179.4	210.2	125.6	1.18	1.18	1.25	1.03	-	-	18	1200/665
		23F	120	405	420.3	231.9	17.5	18.2	10.0	19.4	11.1	15.6	-	-	175.5	182.1	100.5	1.17	1.17	1.18	0.96	-	-	18	1200/665
	Head	1M	80	246.2	178.9	420.3	4.3	3.1	7.3	4.9	3.6	10.8	-	-	43.1	31.3	73.7	0.64	0.44	0.41	0.50	0.35	1.32	26	570/440
		5F	100	344.7	303.1	444.2	12.8	11.2	16.5	11.5	10.1	27.4	-	-	128.3	112.8	165.4	0.72	0.60	0.57	0.66	0.74	1.21	36	630/540
		21M	120	320	321.8	600.6	53.7	54.0	100.9	44.2	44.5	142.1	-	-	537.6	540.6	1009	0.93	0.93	0.93	1.25	-	-	54	650/854
Sensation 16	Body	2M	80	80	92.1	146	2.8	3.2	5.1	2.5	4.6	7.2	2.8	5.2	28	32.2	51.1	0.87	0.70	0.72	0.79	0.7	1.5	7	250
		2F	80	80	81	114.7	2.8	2.83	4.0	2.7	4.0	6.3	2.7	6.3	28	28.3	40.1	1.13	0.91	0.91	0.97	0.5	1.0	7	250
		11 M	120	400	203.7	192.4	15.1	7.70	7.27	25.9	12.5	12.1	23.9	11.5	151.2	77.0	72.7	1.10	1.10	0.86	0.87	-	-	18	1200/665
		11 M	120	400	255	264.8	15.1	9.6	10.0	22.6	14.9	14.6	23.9	15.8	151.2	96.3	100.1	1.10	1.10	0.95	0.96	-	-	18	1200/665
		23M	120	400	468.7	280	15.1	17.7	10.5	15.5	10.8	15.0	-	-	151.2	177.2	105.8	1.10	1.10	1.17	0.97	-	-	18	1200/665
		23F	120	400	415.1	229	15.1	15.6	8.6	16.7	9.5	13.4	-	-	151.2	156.9	86.5	1.10	1.10	1.12	0.91	-	-	18	1200/665
	Head	1M	120	98.3	71.4	167.9	27.6	20.0	47.1	31.9	23.2	69.3	-	-	276.4	200.8	471.8	1.81	1.81	1.59	2.28	-	-	26	570/440
		5F	80	144.2	126.8	185.4	15.4	13.5	19.8	13.8	12.1	32.8	-	-	154	135.4	198	2.13	1.44	1.37	1.58	0.70	1.13	36	630/540
		21M	120	226.7	234.9	425.5	40.1	41.6	75.3	33.0	34.2	106.1	-	-	401.6	416.3	753.8	0.82	0.82	0.83	1.09	-	-	54	650/854

Once the input parameters are entered, and the relevant procedure selections are carried out, the program calculates and displays the output figures in a single window, along with the DRLs as shown in the figure below.

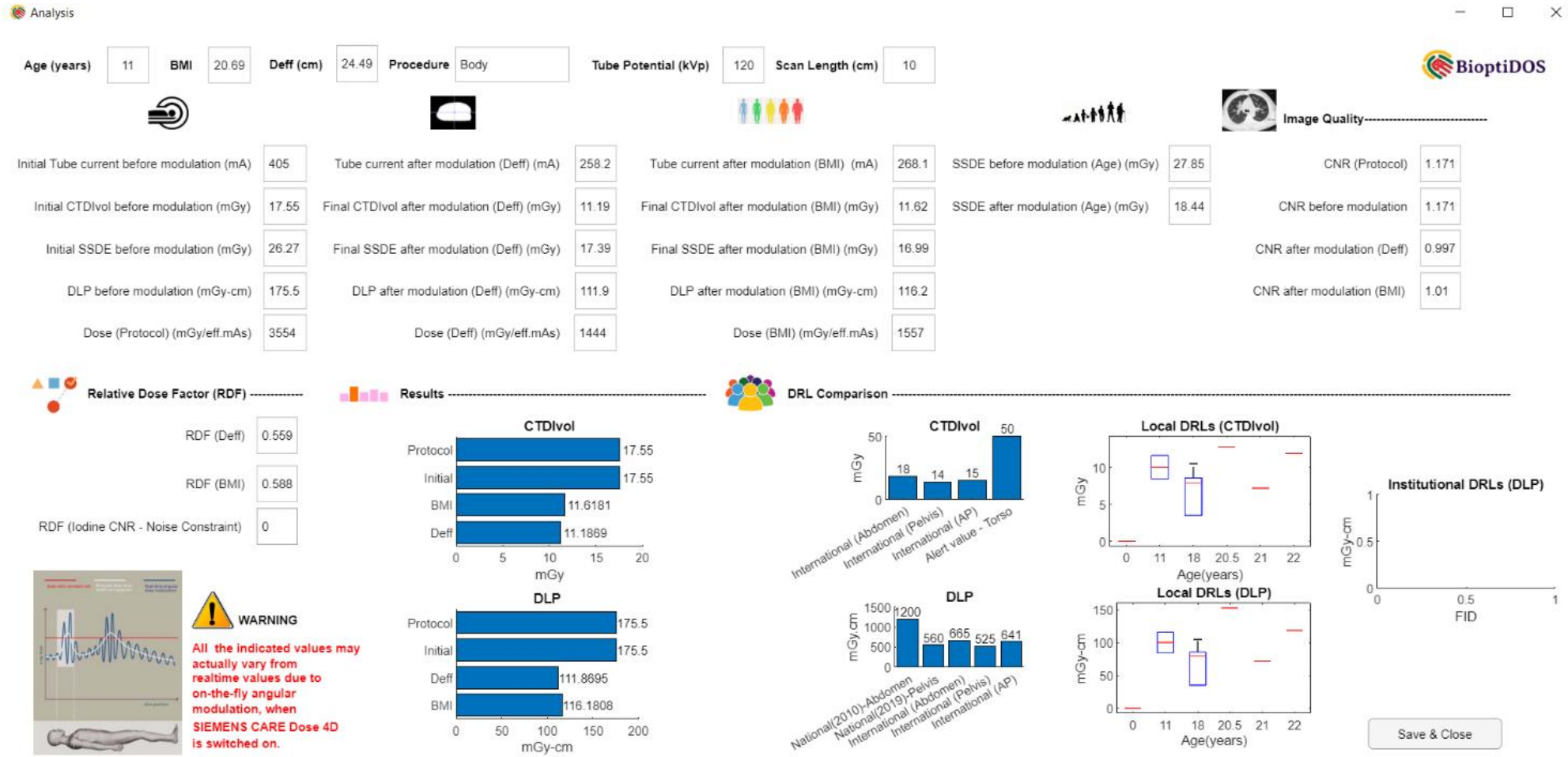

Fig. 6. Results window of the program

The relationship between the distinctive tube parameters and the output can be visualized from the Figure. 7. To be specific the dependency between the $CTDI_{vol}$ and tube potential and current and the age of the patient. Moreover, factors like the specific procedure (Head or Body) and the patient's age, altogether impact the tube output. Both these components decide the suitable phantom to be utilized, E.g., a 16 cm PMMA phantom is chosen for a pediatric patient's head & body procedures and an adult's head strategy, while a 32 cm PMMA phantom is chosen for a well-grown adult's body procedure. In this manner for a given set of tube parameters, the resultant dosage is higher in a 16 cm phantom, when compared to a 32 cm phantom.

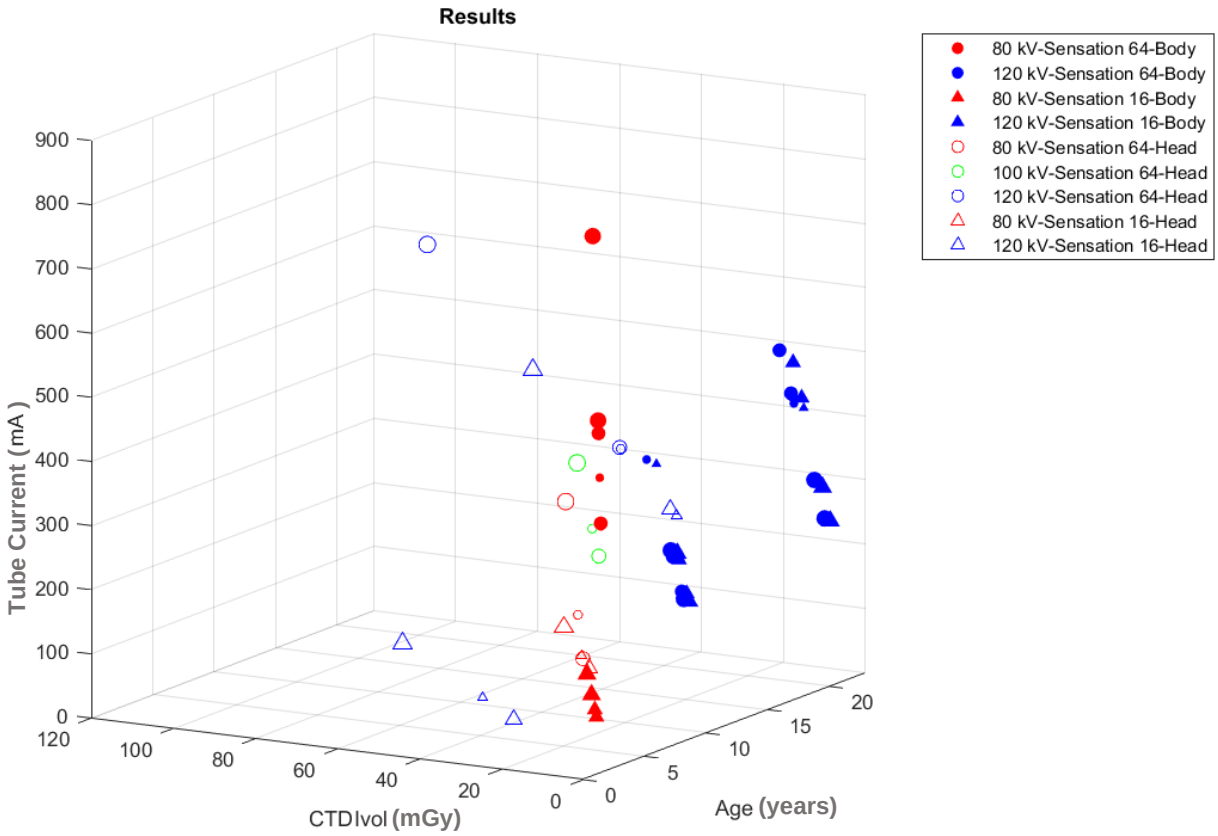

Fig. 7. 3-Dimensional chart (Age Vs Tube current Vs $CTDI_{vol}$)

The relationship between dose and tube potential is of exponential nature which changes concurring to the particular circumstances [2]. The dosage is simply expanded as long as tube current settings are not changed, $CTDI_w$ increment with kV to the power of 2.5, which suggests that both are expanded by around 50% on the off chance that kV is expanded [2]. Moreover, the relationship between the tube current and the dose is directly corresponding, and the dose increases with an increment within the same sum of tube current. It can be seen from Figure. 7, that $CTDI_{vol}$ increases with an increase in phantom size, kV, and tube current.

The tube current alters based on the patient's effective diameter and the BMI was calculated utilizing the CARE Dosage 4D empirical equation given within the previous segment. The lookup table for BMI conversion to effective diameter is given within the Appendix. Based on these transformations the tube current change was obtained and is given in Table. 11 and is plotted in Figure. 7. It is obvious that in most of the cases, the change based on BMI is higher than that of the Deff. This could be

advocated by the reality that BMI accounts for the entire body weight and stature of the patient, whereas D_{eff}, as it were, considers the most remote separations between the AP and LAT measurements of the patient. The authors backed this by expressing that the BMI takes into consideration the tissue attenuation of the patient based on their body habitus of either being lean, normal, obese, underweight, or overweight [11]. Another obvious contrast is the dose from two diverse scanners for the same patient and procedure parameters. The dose from Sensation 64 is less than that of the Sensation 16 scanner, where the no. of detector slices plays a major role in determining the dose [11].

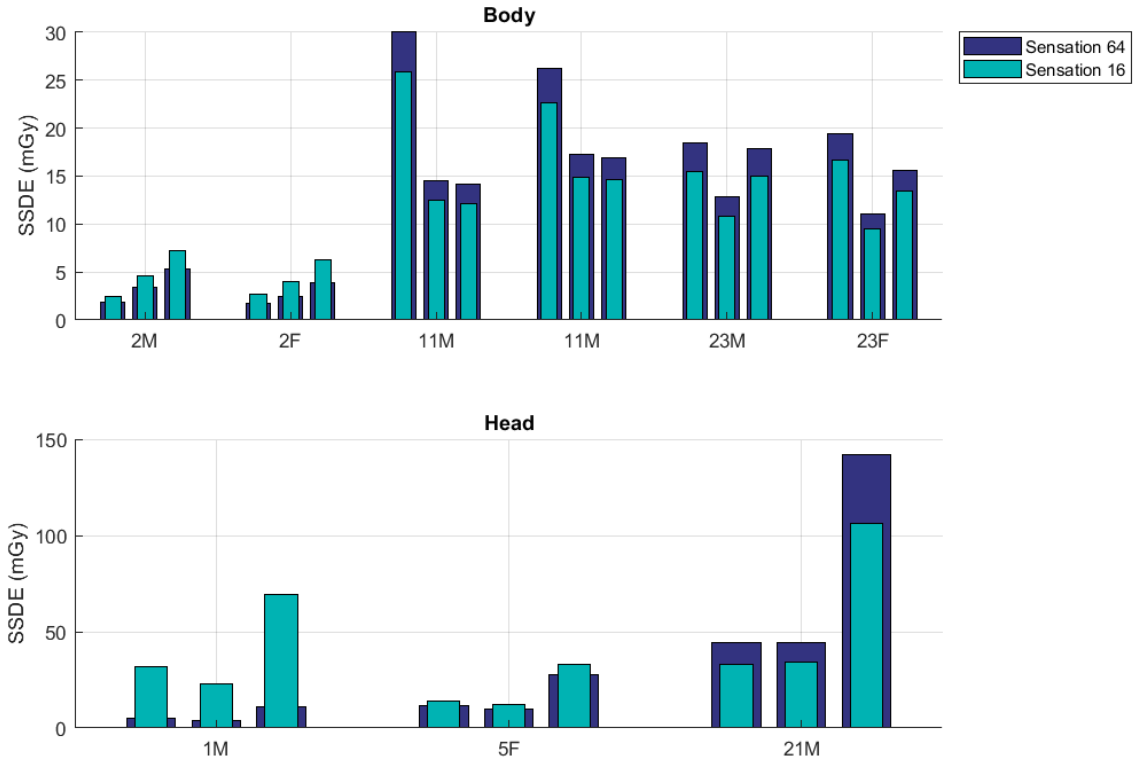

Fig. 8. SSDE for various age groups

The SSDE for all the procedures was calculated by the program using lookup tables for conversion factors and formulae given by the AAPM [8, 9]. The program can compute the SSDE for both the body and head CT procedures, using the factors such as the age, effective diameter, and BMI of the patient. Figure. 8 shows the comparison of SSDE based on protocol, D_{eff}, BMI respectively for all the age groups. It can be seen that SSDE from Sensation 16 is higher than Sensation 64 for pediatric patients for both the body and head procedures. The difference between the SSDE calculated using age and BMI is given in the following table.

Table 12. Difference between $SSDE_{age}$ and $SSDE_{BMI}$

Sl.no.	Patient	Initial SSDE (mGy)	$SSDE_{BMI}$ (mGy)	$SSDE_{age}$ (mGy)	Pecent difference
1.	2M	1.9	5.3	3.8	28.3 %
2.	2M	2.5	7.2	5.2	27.7 %
3.	2F	1.7	3.9	2.5	35.8%
4.	2F	2.7	6.3	6.3	0%
5.	11M	30.1	14.1	13.4	4.9 %
6.	11M	22.6	14.6	15.8	8.2 %
7.	11M	26.2	16.9	18.4	8.8 %
8.	11M	22.6	14.9	15.8	6.04 %

The CNR is used as an indicator for the expected diagnostic image quality. The $CTDI_{vol}$ and the slice thickness can be used to determine the CNR, by using the formula given in the previous section. The higher the CNR for an image, the better is its perceptibility. CNR increases with an increase in the $CTDI_{vol}$, but the dose to the patient should be justified. Therefore the significance for assessment of pre-modulation CNR is realized. Figure. 9. shows the comparison of the CNR for different procedures for a given slice thickness.

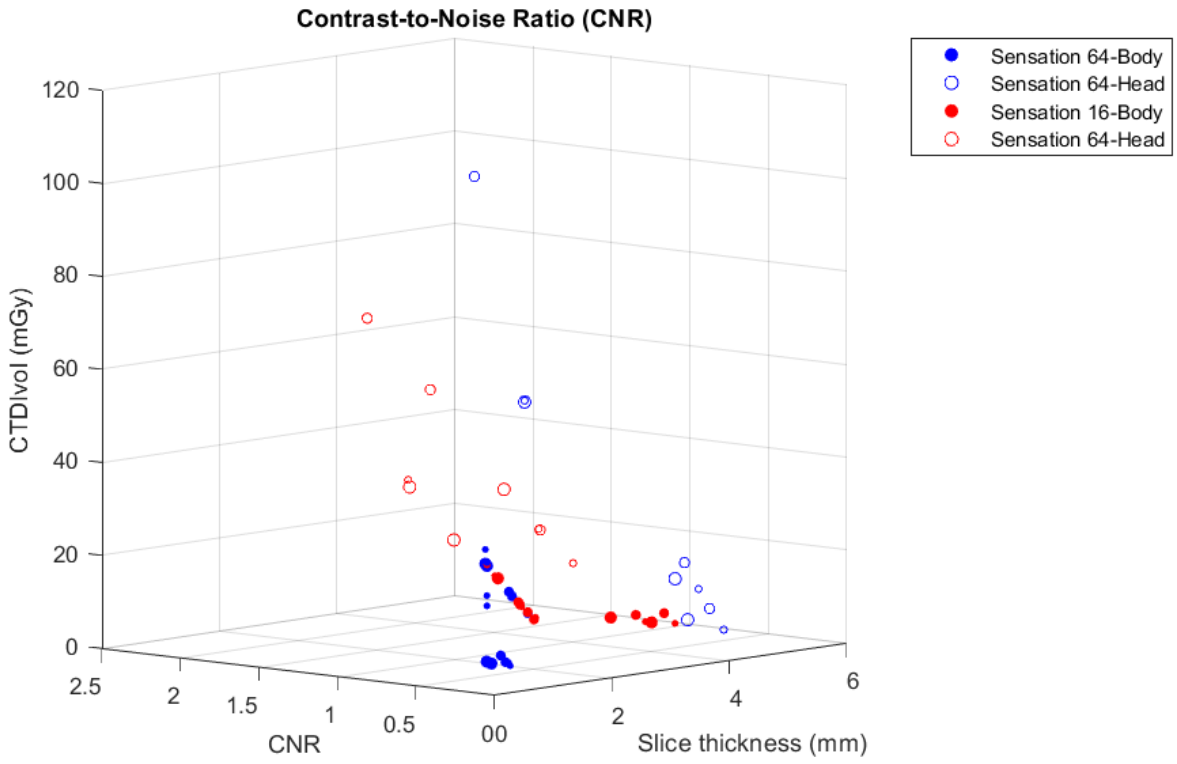

Fig. 9. CNR for various age groups.

The RDF is a quantifier that indicates the amount of radiation dose required/saved while trying to achieve the image quality needed for the protocol, in case if the tube potential is changed. The RDF quantifier can be very helpful in knowing the deviation of the amount of radiation prescribed by the protocol while linking the same with the image quality assessment. The following table shows the RDF calculation for the patients.

Table 13. RDF for different patients

Scanner	Region	Patient	Protocol kV	kV used	RDF - Deff	RDF - BMI
Sensation 64	Body	2M	120	80	0.6 (40%)	1.2 (-20%)
		2F	120	80	0.4 (60%)	0.8 (20%)
	Head	1M	120	80	0.35 (65%)	1.32 (-32%)
		5F	120	100	0.74 (26%)	1.21 (-21%)
Sensation 16	Body	2M	120	80	0.7 (30%)	1.5 (-50%)
		2F	120	80	0.5 (50%)	1.0 (0%)
	Head	5F	120	80	0.7 (30%)	1.13 (-13%)

It is inferred from the above table that, the RDF indicates the amount of tube current is additionally used when a lower kV is used, in case of modulation based on the BMI (indicated using a negative percentage). Also, it can be seen that dose savings occur during modulation based on D_{eff}. This suggests that tube modulation based on BMI results in more dosage to the patient when compared to D_{eff} and RDF could be used as a valid parameter in assessing the deviation between the protocol parameters and actual scan parameters.

3.1. Shortcomings of the prototype program

The program was analyzed using different settings, as discussed in the previous section. The main limitations of the program are listed as follows,

- The prototype is developed using a simple MATLAB script. Since the source code is rhetorical and requires many user selections, the time taken to complete a trial could take up to a few minutes. The nature of this program is navigational, and cannot allow the user to revert to previous selections, once it is chosen.

- Only two scanners were included in the program. Though the reason behind this is well justified, a wide range of scanners are currently used in the CT industry, and therefore largely restricts the program's usability.

- The modeling of the proprietary AEC systems is strictly prohibited, since the replication carried out in the program is based on the empirical equations derived by another author [39], the accuracy of this prediction of tube current changes cannot be well established. The equations only account for longitudinal tube current modulation and not that of angular tube current modulation. Therefore the error levels of this program should be calculated.

- The results based on D_{eff} and BMI modulations are mostly sensible, for most of the body CT procedures, but for head examinations, it is inferred that BMI results are unacceptable.

- The results obtained for various age groups are inconsistent and require further investigation. For example, the tube current levels used for a 2 – year old are higher when compared to a 23 – year old, in few instances, which indicates errors in calculation.

3.2. Practical implementations of the program

To analyze the possibilities of further developing the current prototype program for routine clinical usage in the CT department of hospitals, and to discuss the forthcoming of the implementations, professional advice was sought out. A demonstration of the program was carried out, followed by the consultation held virtually on April 1, 2021, with an expert panel consisting of,

1. Dr. Birutė Griciene, Head, Clinical Radiation Care Division, Vilniaus Universiteto ligoninė Santaros Klinikos, Vilnius.
2. Kirill Skovorodko, Expert Medical Physicist, Vilniaus Universiteto ligoninė Santaros Klinikos, Vilnius.
3. Antonio Jreije, Medical Physicist, Vilniaus Universiteto ligoninė Santaros Klinikos, Vilnius.

After discussions it was agreed by both the panel and the authors, that the prototype program in its current form, requires some improvements, and cannot be strictly implemented for routine clinical examinations, however it has the potential to be implemented for research purposes, when investigating patient dose optimization in Computed Tomography.

Conclusions

1. In this thesis, a MATLAB® based algorithm was proposed and developed, to optimize the patient dose in CT examinations, which takes into account a patient's age, size, shape, etc. It primarily calculates the TCM output of the CT scanner, in terms of tube current, for different approaches of TCM based on D_{eff} and BMI of the patient, along with other age & size-based recommendations of kV_p and mA required for the patient.

2. The program was corroborated for its functionality, with 6 pediatric and 3 adult reference patients having random BMI characteristics such as being lean, normal & obese, for 4 head & abdomen CT clinical protocols of both 64 & 16 slices scanners. To analyze the outcomes of the testing, a total of 360 numerical values in terms of $CTDI_{vol}$, SSDE, CNR, and RDF for three major categories – Initial, D_{eff}, and BMI based TCM approaches, were obtained and analysed.

3. The testing results confirmed the basic inherent physics behind the CT technology, such as the increments and decrements of $CTDI_{vol}$, with respect to factors like kV, phantom size, mAs, pitch, etc. Both SSDE and CNR were dependent on $CTDI_{vol}$, thereby establishing the fact that, prediction of $CTDI_{vol}$ to be critically crucial in CT procedures.

4. Though the testing results indicated sensible estimations for D_{eff} and BMI based TCM methods, few notable exceptions were observed. The results of BMI-TCM approach for all head examinations were rendered unacceptable. Inconsistent results were noticed, at few instances with the 2-year old pediatric patient for abdomen examination, signalling errors in calculation. The accuracy of the sourced data embedded in the program, needs to be established.

5. Practical implementations of the program concept were discussed with clinical professionals and it was agreed that it needs improvements, however it has the potential as a useful research tool when it comes to patients' dose optimization in CT. The source code of the prototype is made open access, for future development of the program, by interested research groups.

Acknowledgements

First and Foremost, I would like to confer my heartiest thanks to my Project Supervisor, Prof. Dr. Diana Adlienė for motivating and guiding me during my study and in the completion of this thesis.

I wish to express my deepest gratitude to Lect. Dr. Choirul Anam of Universitas Diponegoro, Indonesia, for contributing their "IndoseCT" software program, which formed the basis of calculations used in this thesis.

I would like to recognize the invaluable suggestions and guidance provided by Lect. Dr. Benas Gabrielis Urbonavičius and Assoc. Prof. dr. Jurgita Laurikaitienė, in improving this thesis.

I wish to whole-heartedly appreciate Dr. Birutė Griciene, Kirill Skovorodko and Antonio Jreije of Vilniaus Universiteto ligoninė Santaros Klinikos, Vilnius, for taking time to provide their valuable feedback about the developed prototype and its implementation.

List of References.

1. INTERNATIONAL ATOMIC ENERGY AGENCY, *Dose Reduction in CT while Maintaining Diagnostic Confidence: A Feasibility/Demonstration Study*, IAEA-TECDOC-1621, IAEA, Vienna 2009.
2. NAGEL H.D, *CT Parameters that Influence the Radiation Dose*. Radiation Dose from Adult and Pediatric Multidetector Computed Tomography. Medical Radiology (Diagnostic Imaging). Springer, Berlin, Heidelberg, pp 51-79, ISBN 978-3-540-68575-3, 2007.
3. MARTIN, C J, SOOKPENG S. Setting up computed tomography automatic tube current modulation systems. *Journal of Radiological Protection*, 36(3), R74–R95, 2016.
4. TRATTNER S, PEARSON GDN, et al. Standardization and optimization of CT protocols to achieve low dose. *J Am Coll Radiol*.;11(3):271-278, 2014.
5. ZHANG, Y, SMITHERMAN C, SAMEI E. Size-specific optimization of CT protocols based on minimum detectability. *Medical Physics*, 44(4), 1301–1311, 2017.
6. MCKENNEY SE, SEIBERT JA et al. Methods for CT automatic exposure control protocol translation between scanner platforms. *J Am Coll Radiol*.;11(3):285-91, 2014.
7. MCCOLLOUGH CH, LENG S, et al. CT dose index and patient dose: they are not the same thing. *Radiology*.;259(2):311-6, 2011.
8. STRAUSS K, et al. Size Specific Dose Estimates in Pediatric and Adult Body CT Examinations, *AAPM Task Group*, 2014.
9. BOONE J, et al. Size Specific Dose Estimate Head CT, *AAPM Task Group*, 2019.
10. BRINK J, MORIN R. Size-specific Dose Estimation for CT: How Should It Be Used and What Does It Mean?. *Radiology*, 265(3), 666–668, 2012.
11. O'NEILL S, et al. Using body mass index to estimate individualised patient radiation dose in abdominal computed tomography. *European Radiology Experimental*, 2(1), 38, 2018.
12. KAWASHIMA H, et al. Relationship between size-specific dose estimates and image quality in computed tomography depending on patient size. *J Appl Clin Med Phys*.;19(4):246-251, 2018.
13. ANAM C, et al. A fully automated calculation of size-specific dose estimates (SSDE) in thoracic and head CT examinations. *Journal of Physics: Conference Series*, 694, 012030, 2016.
14. SARMENTO S, et al. Automatic calculation of patient size metrics in computed tomography: What level of computational accuracy do we need?. *Journal of Applied Clinical Medical Physics*, 19(1), 218–227, 2018.
15. FAHMI A, ANAM C, et al. Correlation between age and head diameters in the paediatric patients during CT examination of the head, *Polish Journal of Medical Physics and Engineering*, 25(4), 229-235, 2019.
16. INTERNATIONAL COMMISSION ON RADIATION UNITS AND MEASUREMENTS. ICRU Report No. 87: Radiation dose and image-quality assessment in computed tomography. *J ICRU*;12(1):1-149, 2012.
17. SECHOPOULOS I, et al. The DICOM Radiation Dose Structured Report: What It Is and What It Is Not. *J Am Coll Radiol*.;12(7):712-3, 2015.
18. BOOS J, et al. Dose Monitoring in Radiology Departments: Status Quo and Future Perspectives. *Rofo*;188(5):443-50, 2016.
19. RICCARDI L, et al. Use of radiation dose index monitoring software in a multicenter environment for CT dose optimization. *Radiol med* 123, 944–951, 2018.

20. TSAPAKI V, FITOUSI N, et al. Experience with the use of a dose management system in the everyday routine of a CT department. A touchstone or a millstone? *Hell J Radiol*; 3(1): 05-14, 2018.
21. VAÑÓ E, et al. ICRP Publication 135: Diagnostic Reference Levels in Medical Imaging. *Ann ICRP*; 46(1):1-144, 2017.
22. VASSILEVA J, REHANI M. Diagnostic Reference Levels. *American Journal of Roentgenology*, 204(1), W1–W3, 2015.
23. SO¨DERBERG M. Overview, Practical Tips And Potential Pitfalls Of Using Automatic Exposure Control In Ct: Siemens Care Dose 4D. *Radiation Protection Dosimetry*; 169(1-4):84-91., 2015.
24. JAUHARI A, ANAM C, et al. The effect on CT size-specific dose estimates of mispositioning patients from the isocentre. *European Journal of Molecular & Clinical Medicine*, 8, 3, 155-164, 2021.
25. FURUKAWA Y, et al. Inadequate object positioning and improvement of automatic exposure control system calculations based on an empirical algorithm. *Phys Eng Sci Med*, 44, 37–44, 2021.
26. MURUGAN V, et al. American College of Radiology Dose Index Registry. *Journal of Thoracic Imaging*, 30(6), W66–W68, 2015.
27. KEAT N. CT scanner automatic exposure control systems. Available from: doi: 10.13140/RG.2.1.3128.4720, 2005.
28. SÖDERBERG M, Automatic exposure control in CT: an investigation between different manufacturers considering radiation dose and image quality, Available from: http://lup.lub.lu.se/student-papers/record/2157064, 2008.
29. MARTIN C J, SOOKPENG S, Setting up computed tomography automatic tube current modulation systems, *J. Radiol. Prot*. 36 R74, 2016.
30. KHOBRAGADE P, et al. CT automated exposure control using a generalized detectability index. *Med Phys*; 46: 140– 151, 2019.
31. WANG X., et al. Automatic tube potential selection with tube current modulation in coronary CT angiography: Can it achieve consistent image quality among various individuals?. *Experimental and Therapeutic Medicine*, 16, 253-259, 2018.
32. DE MATTIA C, et al. Patient organ and effective dose estimation in CT: comparison of four software applications. *Eur Radiol Exp*; 4(1):14, 2020.
33. ANAM C, et al. Volume computed tomography dose index ($CTDI_{vol}$) and size-specific dose estimate (SSDE) for tube current modulation (TCM) in CT scanning. *Int J Radiat Res*.; 16 (3) :289-297, 2018.
34. MUBAROK S et al. Parameter-based estimation of CT dose index and image quality using an in-house android™-based software, *J. Phys.: Conf. Ser*. 694 012037, 2016.
35. KATSARI K, et al. Establishing a dose management strategy in Computed Tomography, Proceedings. *EuroSafe Imaging*, ESI-0022, Available from: 10.1594/esi2018/ESI-0022, 2018.
36. OSMAN N D, et al. Radiation dose management in CT imaging: Initial experience with commercial dose watch software, *J. Phys.: Conf. Ser*. 1497 012020, 2020.
37. VALSTYBINĖ AKREDITAVIMO SVEIKATOS PRIEŽIŪROS VEIKLAI TARNYBA, Kompiuteriniai Tomografai – 2019; Brangioms sveikatos priežiūros technologijoms, Retrieved from:https://vaspvt.gov.lt/files/Brangus_medicinos_prietaisai/KT_2020%20%282019%20m.%20duomenys%29.pdf , 2020.

38. MCNITT-GRAY M, Tube current modulation approaches: overview, practical issues and potential pitfalls, *AAPM 2011 Summit on CT Dose, 2011,* Retrieved from: www.aapm.org/meetings/2011CTS/documents/McNitt-GrayTubeCurrentModulationv4.pdf.
39. MACDOUGALL RD, et al. Size-based protocol optimization using automatic tube current modulation and automatic kV selection in computed tomography. *J Appl Clin Med Phys*.;17(1):328-341, 2016.
40. SÖDERBERG M, GUNNARSSON M, The effect of different adaptation strengths on image quality and radiation dose using Siemens Care Dose 4D, *Radiation Protection Dosimetry*, Volume 139, Issue 1-3, Pages 173–179, 2010.
41. Kesh Ikuma, inputsdlg: Enhanced Input Dialog Box Available from: (https://www.mathworks.com/matlabcentral/fileexchange/25862-inputsdlg-enhanced-input-dialog-box), *MATLAB Central File Exchange*. Retrieved on March 15, 2021.
42. MCCOLLOUGH CH, Translating Protocols Across Patient Size: Babies to Bariatric, Technology Assessment Initiative, *AAPM 2011 Summit on CT Dose, 2011*. Retrieved from: https://www.aapm.org/meetings/2011CTS/documents/McCollough_BabiestoBariatric2011.pdf.
43. DIEGO L, et al. Tube Potential and CT Radiation Dose Optimization. *American Journal of Roentgenology*, 204(1), W4–W10, 2015.
44. GOLDMAN L W. Principles of CT: Multislice CT. *J Nucl Med Technol*; 36(2):57-68, 2008.
45. MCCOLLOUGH C, et al. Use of Water Equivalent Diameter for Calculating Patient Size and Size-Specific Dose Estimates (SSDE) in CT: The Report of AAPM Task Group 220. *AAPM Rep*. 2014;2014:6-23.
46. SIEGEL MJ, et al. Automated low-kilovoltage selection in pediatric computed tomography angiography: Phantom study evaluating effects on radiation dose and image quality. *Invest Radiol*; 48(8):584-9, 2013.
47. LIFENG YU, et al. Automatic selection of tube potential for radiation dose reduction in CT: A general strategy. *Medical Physics*, 37(1), 234, 2010.
48. WIKIPEDIA CONTRIBUTORS. Body mass index. In *Wikipedia, The Free Encyclopedia*. Retrieved from: https://en.wikipedia.org/w/index.php?title=Body_mass_index&oldid=1022022978, on 17 March 2021.
49. ELLIOT K. FISHMAN, MD, CTisus.com, Available from: https://www.ctisus.com, Accessed 17 Mar. 2021.
50. VRAD - VIRUTAL RADIOLOGIC, Available from: https://www.vrad.com, Accessed 17 Mar. 2021.
51. UT SOUTHWESTERSN MEDICAL CENTER, Department of Radiology, Available from: https://www.utsouthwestern.edu, Accessed 17 Mar. 2021.
52. LIFESPAN BY RHODE ISLAND HOSPITAL AND THE MIRIAM HOSPITAL, Available from: https://www.lifespan.org, Accessed 17 Mar. 2021.
53. OREGON HEALTH & SCIENCE UNIVERSITY - OHSU, Diagnostic Radiology, Available from: https://www.ohsu.edu, Accessed 17 Mar. 2021.
54. TRA MEDICAL IMAGING, Available from: https://www.tranow.com, Accessed 17 Mar. 2021.
55. DARTMOUTH GEISEL SCHOOL OF MEDICINE, DEPARTMENT OF RADIOLOGY, Available from: https://geiselmed.dartmouth.edu, Accessed 17 Mar. 2021.
56. REID J, et al. Optimization of kVp and mAs for Pediatric Low-Dose Simulated Abdominal CT: Is It Best to Base Parameter Selection on Object Circumference?. *AJR Am J Roentgenol*;195(4):1015-20, 2010.

57. PYFFEROEN, L, et al. Benchmarking adult CT-dose levels to regional and national references using a dose-tracking software: a multicentre experience. *Insights Imaging* 8, 513–521, 2017.
58. SAKHNINI L, CT radiation dose optimization and reduction for routine head, chest and abdominal CT examination. *Radiol Diagn Imaging* 2:1-4, ISSN: 2515-0200, 2017.
59. JA¨RVINEN, H, et al. Indication based national diagnostic reference levels for paediatric CT: a new approach with proposed values. *Radiat. Prot. Dosim*. 165, 86–90, 2015.
60. SAMEI E, CHRISTIANSON O, Dose index analytics: more than a low number. *J. Am. Coll. Radiol*. 11, 832–834, 2014.
61. MOHAMAD FAWZI AWAD et al, A systematic review on the current status of adult diagnostic reference levels in head, chest and abdominopelvic Computed Tomography, *J. Radiol. Prot*. 40 R71, 2020.
62. VASSILEVA, J. et al, A study to establish international diagnostic reference levels for paediatric computed tomography. *Radiation Protection Dosimetry*, 165(1-4), 70–80, 2015.
63. EUROPEAN COMMISSION, DDM2 Project Report Part-2, Diagnostic Reference Levels (DRLs) in Europe, Retrieved from: ENER/2010/NUCL/SI2.581237, 2010.
64. RADIACINĖS SAUGOS CENTRAS, RSC Annual Report 2012, Retrieved from: https://www.rsc.lt/index.php/pageid/428, Vilnius, 2012.
65. RADIACINĖS SAUGOS CENTRAS, RSC Annual Report 2015, Retrieved from: https://www.rsc.lt/index.php/pageid/428, ISSN 2351-5953, Vilnius, 2015.
66. RADIACINĖS SAUGOS CENTRAS, RSC Annual Report 2019, Retrieved from: https://www.rsc.lt/index.php/pageid/428, ISSN 2351-5953, Vilnius, 2019.

Appendices

Appendix 1. Accessibility to the program

BioptiDOS was written using MATLAB® - R2020b v.9.9.0 (The MathWorks Inc.), incorporating various functions. It is a semi-open-source estimator for exposure control in diagnostic CT procedures and an SSDE calculator based on patient biometrics. This program is for educational purposes and strictly not intended for clinical uses. The authors nor their affiliated institution assumes responsibility for the usage of this program. Users are requested not to solely rely on the accuracy of the data herein. Any and all liability and damages arising directly from using this application are hereby disclaimed. The information herein is provided "as is" and without any warranty expressed or implied. Please use the program at your discretion.

The target system should have the latest version of MATLAB® (preferably R2018a or later), along with Image Processing Toolbox™ since the program deals with analyzing the DICOM images. The contents of the folder should not be altered, and it is necessary to have all the files in a single folder for the proper execution of the code.

The weblink to download the folder containing the Master code, along with its auxiliary functions and databases is provided as follows,

https://drive.google.com/drive/folders/1dYQZEQkpYq_x3VbJXvtWBUNfm3pUXSC_?usp=sharing

To use the program, download the folder, add it to the current path, and then open and run the MATLAB file named, "*Bioptidos_Main_Script.m*". The instructions on how to work with this program is provided in Section 2.4 of this document.

Appendix 2. CT Protocols

Table A 1. List of CT Protocols embedded in the program

Scanner	Age	Region	Protocol ID	Protocol name
Sensation 64	Adult	Abdomen	S64A11	Abdomen CTA mesentery: Ischemic bowel
			S64A12	Abdomen CTA: Pancreas 3D
			S64A13	Abdominal/Pelvic Trauma
			S64A14	Adrenal: incidentaloma
			S64A15	Adrenal: stage adrenal cancer
			S64A16	Bony pelvis
			S64A17	Colon: Virtual colonoscopy
			S64A18	Kidney: Hematuria
			S64A19	Kidney: Mass (staging)
			S64A110	Kidney: R/o mass
			S64A111	Kidney: Renal donor
			S64A112	Kidney: Renal stone
			S64A113	Large Patient 3D
			S64A114	Liver: Evaluate or r/o mass
			S64A115	Pelvic mass or tumor staging
			S64A116	R/O appendicitis
			S64A117	R/O Diverticulitis
			S64A118	Routine Abdomen: R/O abscess
			S64A119	Routine Pelvis: (R/O abscess, mass, etc.)
			S64A120	Small bowel: Crohn's disease
			S64A121	Small bowel: R/o ischemic bowel
			S64A122	Whole body screening with cardiac
		Cardiac	S64A21	Calcium score (spiral)
			S64A22	Cardiac Routine .33: Coronary arteries
			S64A23	Coronary arteries: Bypass graft patency
			S64A24	Coronary arteries: Stent patency
			S64A25	Coronary CTA
			S64A26	Low Heart Rate .37 : Coronary arteries
		Chest	S64A31	Aorta
			S64A32	Aorta: Trauma
			S64A33	Chest (airway)
			S64A34	Chest Abd routine (R/O masses stage lymphoma)
			S64A35	Chest CT- R/O Malignancy
			S64A36	Chest CT: HRCT Routine Spiral
			S64A37	Chest CT: Lung Cancer Screening
			S64A38	Chest CT: Stage Malignancy
			S64A39	Chest: PE Study Routine Spiral
			S64A310	Hi Res Chest (ILD)
			S64A311	PE study
			S64A312	R/O AVM
			S64A313	R/O Occupational disease (asbestosis)
			S64A314	R/O Occupational lung disease (asbestosis screening)
			S64A315	R/O Occupational lung disease (silicosis/cwp)
			S64A316	Routine (R/O mass)
			S64A317	SVC Occlusion
			S64A318	Trauma
		GI Tract	S64A41	GI CT: Crohns Disease
			S64A42	GI CT: Enterography
			S64A43	GI CT: R/O Appendicitis
			S64A44	GI CT: R/O Cholangiocarcinoma
			S64A45	GI CT: R/O GI Bleed
			S64A46	GI CT: R/O Mesenteric Ischemia
			S64A47	GI CT: R/O Small Bowel Obstruction
		Head	S64A51	CT Venogram
			S64A52	CTA
			S64A53	Facial Bones
			S64A54	Temporal Bone
			S64A55	R/O Bleed (Routine Spiral)
			S64A56	Shunt F/U (Sequential)
			S64A57	Sinus CT: R/O Mass
			S64A58	Sinus CT: R/O Sinusitis

		Kidney	S64A61	Hematuria
			S64A62	Mass Staging
			S64A63	R/O Stone
			S64A64	Renal Artery Stenosis
			S64A65	Renal Infection
			S64A66	Renal Vein Thrombosis
			S64A67	Urogram
			S64A68	Kidney- Renal Donor
		Musculoskeletal	S64A71	MSK CT: Shoulder CT
			S64A72	Bone: Foot
			S64A73	Bone: Wrist
			S64A74	C-spine Trauma
			S64A75	Lower Extremity
			S64A76	Lower extremity: Runoff
			S64A77	Mass/Trauma
			S64A78	MSK CT: Lower Extremity Bone
			S64A79	MSK CT: Lower Extremity UHR
			S64A710	MSK CT: Upper Extremity UHR
			S64A711	MSK: Boney Pelvis
			S64A712	Upper Extremity
			S64A713	Vascular CT: Upper Extremity CTA
		Neck	S64A81	Carotid CTA: Carotid stenosis
			S64A82	Internal auditory canal (IAC)
			S64A83	Carotid CTA
			S64A84	Neck CT: Swelling/Mass
			S64A85	Pediatric: Mass or abscess
			S64A86	R/O jugular vein thrombosis
			S64A87	R/O mass or nodes or abscess
		Oncology	S64A91	Bladder Cancer
			S64A92	Breast Cancer
			S64A93	Cervical Cancer
			S64A94	Colon Cancer
			S64A95	Gastric Cancer
			S64A96	Lung Cancer
			S64A97	Lymphoma
			S64A98	Ovarian Cancer
			S64A99	Prostate Cancer
			S64A910	Rectal Cancer
			S64A911	Renal Cell Carcinoma
			S64A912	Transitional Cell Carcinoma
		Pancreas	S64A101	R/O Mass
			S64A102	R/O Pancreatitis
			S64A103	Cyst Follow Up
		Spine	S64A1101	C-Spine
			S64A1102	L-Spine
			S64A1103	T-spine
		Vascular	S64A1201	DIEP FLAP (Vessel Mapping)
			S64A1202	IVC Thrombosis
			S64A1203	Lower Extremity CTA
			S64A1204	Trauma Abdomen CTA
			S64A1205	Aorta (Routine Spiral)
			S64A1206	Aorta Stent (Routine Spiral)
	Pediatric	Abdomen	S64P11	Abdomen
		Bone	S64P21	Spine
		Chest	S64P31	HRCT Chest
		Head	S64P41	Head CT (Routine Spiral)
			S64P42	R/O Sinusitis
			S64P43	Temporal Bone
			S64P44	Shunt F/U (Sequential)
		Neck	S64P51	Neck CT

Sensation 16	Adult	Abdomen	S16A11	AbdRoutine (R/O abscess, FUO, etc.)
			S16A12	Adrenal Gland: Mass
			S16A13	Aorta
			S16A14	Aorta: F/u stent placement
			S16A15	Aorta: Pre-operative AAA evaluation
			S16A16	Bladder
			S16A17	Colon
			S16A18	Gyn: Oncology 3D Protocol
			S16A19	Kidney (CT urography)
			S16A110	Kidney (Hematuria)
			S16A111	Kidney (Mass)
			S16A112	R/O jugular vein thrombosis
			S16A113	R/O mass or nodes or abscess
			S16A114	Bladder Cancer
			S16A115	Breast Cancer
			S16A116	Cervical Cancer
			S16A117	Colon Cancer
			S16A118	Gastric Cancer
			S16A119	Lung Cancer
			S16A120	Lymphoma
			S16A121	Ovarian Cancer
			S16A122	Prostate Cancer
		Cariothoracic	S16A21	Rectal Cancer
			S16A22	Renal Cell Carcinoma
			S16A23	Transitional Cell Carcinoma
			S16A24	R/O Mass
			S16A25	R/O Pancreatitis
			S16A26	Cyst Follow Up
			S16A27	C-Spine
			S16A28	L-Spine
			S16A29	T-spine
		Head	S16A30	DIEP FLAP (Vessel Mapping)
			S16A31	IVC Thrombosis
			S16A32	Lower Extremity CTA
			S16A33	Trauma Abdomen CTA
			S16A34	Aorta (Routine Spiral)
			S16A35	Aorta Stent (Routine Spiral)
			S16A36	Abdomen
		Musculoskeletal	S16A41	Spine
			S16A42	HRCT Chest
			S16A43	Head CT (Routine Spiral)
			S16A44	R/O Sinusitis
			S16A45	Temporal Bone
		Neck	S16A51	Shunt F/U (Sequential)
			S16A52	Neck CT
			S16A53	AbdRoutine (R/O abscess, FUO, etc.)
	Pediatric	Abdomen	S16P11	Adrenal Gland: Mass
			S16P12	Aorta
		Bone	S16P21	Aorta: F/u stent placement
		Chest	S16P31	Aorta: Pre-operative AAA evaluation
			S16P32	Bladder
			S16P33	Colon
		Head	S16P41	Gyn: Oncology 3D Protocol
			S16P42	Kidney (CT urography)
			S16P43	Kidney (Hematuria)
			S16P44	Kidney (Mass)
			S16P45	Inner Ear Studies
			S16P46	Routine Head Study (Spiral)
			S16P47	Sequential Study
		Neck	S16P51	Carotid CTA
			S16P52	Neck Routine

Appendix 3. SSDE conversion factors

Table A 2. AP+LAT Conversion factors for 32 cm PMMA phantom [8]

AP + LAT Dimensions (cm)	Effective diameter (cm)	Conversion factor
16	7.7	2.79
18	8.7	2.69
20	9.7	2.59
22	10.7	2.5
24	11.7	2.41
26	12.7	2.32
28	13.7	2.24
30	14.7	2.16
32	15.7	2.08
34	16.7	2.01
36	17.6	1.94
38	18.6	1.87
40	19.6	1.8
42	20.6	1.74
44	21.6	1.67
46	22.6	1.62
48	23.6	1.56
50	24.6	1.5
52	25.6	1.45
54	26.6	1.4
56	27.6	1.35
58	28.6	1.3
60	29.6	1.25
62	30.5	1.21
64	31.5	1.16
66	32.5	1.12
68	33.5	1.08
70	34.5	1.04
72	35.5	1.01
74	36.5	0.97
76	37.5	0.94
78	38.5	0.9
80	39.5	0.87
82	40.5	0.84
84	41.5	0.81
86	42.5	0.78
88	43.5	0.75
90	44.5	0.72

Table A 3. AP+LAT Conversion factors for 16 cm PMMA phantom [8]

AP + LAT Dimensions (cm)	Effective diameter (cm)	Conversion factor
12	5.7	1.5
13	6.2	1.47
14	6.7	1.44
15	7.2	1.42
16	7.7	1.39
17	8.2	1.36
18	8.7	1.34
19	9.2	1.31
20	9.7	1.29
21	10.2	1.26
22	10.7	1.24
23	11.2	1.22
24	11.7	1.19
25	12.2	1.17
26	12.7	1.15
27	13.2	1.13
28	13.7	1.1
29	14.2	1.08
30	14.7	1.06
31	15.2	1.04
32	15.7	1.02
33	16.2	1
34	16.7	0.98
35	17.2	0.97
36	17.6	0.95
37	18.1	0.93
38	18.6	0.91
39	19.1	0.89
40	19.6	0.88
42	20.6	0.84
44	21.6	0.81
46	22.6	0.78
48	23.6	0.75
50	24.6	0.72
52	25.6	0.7
54	26.6	0.67
56	27.6	0.64
58	28.6	0.62
60	29.6	0.6
62	30.5	0.57
64	31.5	0.55
66	32.5	0.53
68	33.5	0.51
70	34.5	0.49
72	35.5	0.47
74	36.5	0.46
76	37.5	0.44
78	38.5	0.42
80	39.5	0.41
82	40.5	0.39

Table A 4. Age based effective diameters [8]

Patient Age (years)	D_E (cm)
0.2	12.1
0.4	13.1
0.6	13.9
0.8	14.6
1	15.1
1.2	15.6
1.4	16
1.6	16.3
1.8	16.6
2	16.8
2.5	17.3
3	17.6
3.5	17.9
4	18.1
4.5	18.3
5	18.5
6	19
7	19.6
8	20.2
9	20.9
10	21.6
11	22.4
12	23.2
13	24.1
14	25
15	26
16	27
17	28.1
18	29.2

Table A 5. BMI based conversion factors for SSDE calculation [11]

BMI	D_E (cm)	$CTDI_{vol}$/SSDE conversion factor
15	20.8	1.73
16	21.6	1.68
17	22.3	1.63
18	23.1	1.59
19	23.8	1.54
20	24.6	1.5
21	25.4	1.46
22	26.1	1.42
23	26.9	1.38
24	27.6	1.34
25	28.4	1.31
26	29.2	1.27
27	29.9	1.23
28	29.9	1.2
29	30.7	1.17
30	31.4	1.14
31	32.2	1.1
32	33	1.07
33	33.7	1.04
34	34.5	1.02
35	35.2	0.99
36	36	0.96
37	36.8	0.93
38	37.5	0.91
39	38.3	0.88
40	39	0.86
41	40.6	0.84
42	41.3	0.81
43	42.1	0.79
44	42.8	0.77
45	43.6	0.75
46	44.4	0.73
47	45.1	0.71
48	45.9	69
49	46.6	0.67
50	47.4	0.65